7-1-2012

Identification of the wings apart transcriptional unit in Drosophila melanogaster

Ginny Morriss

Ginny R. Morriss
Candidate

Biology
Department

This dissertation is approved, and it is acceptable in quality and form for publication:

Approved by the Dissertation Committee:

Richard M. Cripps, Chairperson

Stephen A. Stricker

Cristina D. Takacs-Vesbach

William M. Gelbart

IDENTFICATION OF THE *WINGS APART* TRANSCRIPTIONAL UNIT IN *DROSOPHILA MELANOGASTER*

by

GINNY R. MORRISS

Bachelor of Science, Biology, Gonzaga University, 2007

DISSERTATION

Submitted in Partial Fulfillment of the
Requirements for the Degree of

Doctor of Philosophy

Biology

The University of New Mexico
Albuquerque, New Mexico

July, 2012

ACKNOWLEDGMENTS

I would like to sincerely thank my advisor, Dr. Richard M. Cripps, D. Phil., for his continued support throughout my graduate training. His guidance and encouragement has not only helped me succeed in my graduate education but will remain with me as I progress further into my career.

I also acknowledge the other members of my dissertation committee, Dr. Stephen A. Stricker, Dr. Cristina D. Takacs-Vesbach, and Dr. William M. Gelbart, for their input and recommendations regarding the research presented in this dissertation.

Special thanks to the funding agency and funding programs that have supported my research. Support for this research is provided by the National Institutes of Health. I was also supported through the UNM Initiatives to Maximize Student Diversity program (P.I. Dr. Margaret Werner-Washburne) and More Graduate Education at Mountain States Alliance program sponsored by Arizona State University.

In addition, I would like to thank two very talented undergraduate students, Carmelita Jaramillo and Crystal Mikolajczak for their assistance in maintaining the flies used in this study and their contributions to collecting data from the experiments herein.

Finally, I would like to thank all of my family and friends for the love and support they provided while I pursued my graduate education.

IDENTIFICATION OF THE *WINGS APART* TRANSCRIPTIONAL UNIT IN *DROSOPHILA MELANOGASTER*

by

Ginny R. Morriss

Bachelor of Science, Biology, Gonzaga University

Doctor of Philosophy, Biology, University of New Mexico

ABSTRACT

Muscle development is an evolutionarily conserved process. Mechanisms that govern the development of specific muscles in invertebrates can inform our understanding of how vertebrate muscles form. Understanding these processes allows us to translate developmental mechanisms to disease pathogenesis, as similar genes and developmental processes are affected by these diseases. In this dissertation, *CG14614* is identified as the gene responsible for the *wings apart* phenotype in *Drosophila melanogaster*. This mutation leads to a loss of the adult jump muscle (TDT) in most cases and a greater than 60% reduction in muscle fibers in its least severe form. *wap* mutants fail to properly form neuromuscular junctions to the TDT, resulting in degeneration of the muscle.

Regulation of *Myocyte enhancer factor 2* (*Mef2*) expression in the developing mesoderm, which gives rise to somatic, visceral, and cardiac muscle, by the transcription factors Twist and Mad was also investigated. Our results indicate these are both involved in regulation of the *Mef2* enhancer but additional complexity exists in its regulation that remains to be fully elucidated.

TABLE OF CONTENTS

LIST OF FIGURES

CHAPTER 1

CHAPTER 2

LIST OF TABLES

CHAPTER 1

INTRODUCTION

The study of myogenesis is critically important to understand the function and maintenance of specific muscles, failure of which can lead to muscular dystrophies. These diseases are primarily characterized by skeletal muscle wasting and weakness of varying distribution and severity (Campbell, 1995 and Emery, 2002). Such diseases can result from specific genetic defects common to all muscle cell nuclei, yet in many cases selectively affect individual muscles throughout the body (Lamminen, 1990). The selective effects on different muscles or muscle groups make management of the disease in specific individuals dependent on the type and severity of dystrophy (Emery, 2002). Mutations in specific genes associated with muscular dystrophies have been identified and protein products from these genes are being analyzed in several animal models (Campbell, 1995). This research has shown that common understanding of the molecules and mechanisms involved in muscular dystrophies has been oversimplified and further analyses are necessary to understand the disease mechanisms (Emery, 2002).

The mechanisms involved in invertebrate muscle development are similar to those for vertebrate muscle formation, making the animal model *Drosophila melanogaster* well suited for studies of myogenesis (Baylies and Michelson, 2001). In flies, the basic patterning and specification of the somatic, or skeletal, musculature is similar for all muscle fibers. Moreover, early embryonic myogenesis in *Drosophila* is completed within a few hours (Bate, 1990). These facts, alongside the utility of *Drosophila* to apply a genetic approach to the study

of biological processes, make this system highly amenable to uncovering basic and broadly relevant aspects of muscle development.

The mechanisms of *Drosophila* muscle development occur as a series of consecutive events. The outcome of each event is usually the measure through which the investigator assesses the extent of myogenesis in wild-type and mutant combinations.

Prior to formation of the somatic musculature, the mesoderm must first be specified. This specification of this germ layer is determined by expression of the *dorsal* (FBgn0260632) group genes along the dorsoventral axis of the embryo, which leads to activation of genes such as *twist* (FBgn0003900) and *snail* (FBgn0003448, Leptin, 1991, and Jiang *et al*., 1991). *twist* and *snail* are expressed in cells of the ventral side of the embryo. The *snail* expressing cells give rise to the presumptive mesoderm that invaginates immediately upon reaching a critical threshold of *twist* expression (Leptin *et al.*, 1992). This first phase of mesoderm invagination is achieved in less than twenty minutes and forms a tube of cells through a process of cell shape changes, creating what is known as the ventral furrow (Kam *et al.,* 1991). Formation of the mesoderm occurs when cells from the presumptive mesoderm tube disperse and spread into a single layer of cells over the ventral ectoderm (Leptin, *et al*., 1991). At this point, *snail* expression is not longer detected, but *twist* expression persists (Kosman *et al*., 1991).

Following specification, the mesoderm becomes segmented along both the dorsoventral axis and the anteroposterior axis of the embryo. The gradient of

Dorsal protein established at the onset of embryogenesis along with ectodermal signal induction by *decapentaplegic* (*Dpp*, FBgn0000490) and *wingless* (*wg*, FBgn0004009) signaling leads to activation of genes necessary for dorsoventral segmentation of the mesoderm. High concentrations of Dorsal protein are found at the ventral side of the embryo and activate genes such as *twi*. Dpp is required for induction of the dorsal mesoderm segregation by activating genes like *bagpipe* (*bap*, FBgn0004862) and maintaining levels of *tinman* (*tin*, FBgn0004110) dorsally and repressing ventrally expressed genes, (reviewed in Maqbool and Jagla, 2007). The signal induction allows the dorsal mesoderm to form the midgut visceral mesoderm, dorsal muscles, and heart (Azpiazu and Frasch, 1993, Bodmer, 1993, Azpiazu *et al*., 1996). This regional dorsoventral subdivision of the mesoderm is conserved from invertebrates and vertebrates (reviewed in Azpiazu and Frasch 1993).

After segmentation of the dorsoventral compartments, the mesoderm is organized into parasegmental units with anterior and posterior portions adopting different developmental fates (Azpiazu *et al*., 1996). Cells in the posterior portion of the parasegments express high levels of *twist*, ultimately leading to formation of the somatic musculature (Azpiazu *et al.* 1996, Baylies and Bate, 1996, Castanon *et al.*, 2001, and Furlong *et al*., 2001) by activation of myogenic regulators such as *Myocyte enhancer factor 2* (*Mef2*, FBgn0011656) (Lilly *et al*., 1995). A small population of high Twist-expressing cells postpones differentiation and is set aside for adult muscle development during pupal metamorphosis. These cells are situated at very specific locations, associated with the peripheral

nerves of the abdomen and imaginal discs of the thorax, and prespecify the pattern of the adult musculature (reviewed in Roy and VijayRaghavan, 1999). In the remainder of these cells, *twist* expression decreases and allows for differentiation of the embryonic musculature (Baylies and Bate, 1996).

Following subdivision of the mesoderm, embryonic skeletal muscle development initiates upon specification of a unique founder cell (FC) for each skeletal muscle fiber, and the genetic segregation of that cell from unspecified fusion-competent myoblasts (FCMs) within the mesoderm (Bate, 1990). FCs are specified by the Ras signaling pathway (Artero et al., 2004, Stute et al., 2004) and are differentiated from FCMs by expression of specific genetic markers, such as *Kin of Irre*/*Dumbfounded* (FBgn0028369), *Roughest*/*Irregular Chiasm* (FBgn0003285), and *Rolling Pebbles*/*Antisocial* (FBgn0041096). The FCs then attract the unspecified FCMs to the site of muscle formation, for fusion to generate precursors of the individual muscles of the somatic musculature (reviewed in Chen and Olson, 2004). The FCs are critical determinants of muscle fate. It is widely thought that the FC is responsible for conferring upon the resulting muscle many of the characteristics unique to that muscle: sites of muscle attachment to the cuticle, orientation of the muscle in the embryo, and muscle size (Rushton et al., 1995).

Following specification of FCs and FCMs, myoblast fusion is mediated by genetic factors governing orientation, adhesion, and eventually fusion of the cells to form myotubes (reviewed in Haralalka et al. 2010). The fusion process includes FC-specific markers as well as FCM-specific markers, such as *Sticks*

and Stones (FBgn0024189), *Hibris* (FBgn0029082), and *Lame Duck* (FBgn0039039) (Artero et al., 2004). Other markers expressed during myoblast fusion are molecules of the Rac GTPase signaling pathway and the Ras activator *myoblast city* (FBgn0015513, Laurin et al., 2008), *Loner* (FBgn0026179), *kette* (FBgn0011771, Menon et al., 2005), and *blown fuse* (FBgn0004133, Schroter et al., 2004). Multiple rounds of fusion between FCs and FCMs are required for growth of muscles in the embryo (Bate, 1990, Menon et al., 2005). Cues from the overlying ectoderm, such as secretion of Dpp and wg proteins are also necessary for specification of cell type, myoblast fusion and differentiation (Bate, 1990, Rushton et al., 1995, Currie and Bate, 1991, and Baylies et al., 1995).

Specific muscle gene sets are selectively activated in the individual myoblasts and myotubes by myogenic regulatory proteins such as MEF2 (Sandmann et al., 2006), including the contractile proteins Myosin heavy chain, Troponins I, T, and C, and muscle-specific actins (Arbeitman *et al.*, 2002, Lin et al., 1996, Kelly et al., 2002, and Kelly Tanaka et al., 2008). Accumulation of these contractile proteins, or their mRNA transcripts is indicative of terminal muscle differentiation and are expressed synchronously with genes expressed in the central nervous system (Arbeitman *et al.* 2002).

During the larval stage, muscles specified in the embryo undergo a profound degree of hypertrophy, without overt addition of new myoblasts, nor of nuclear division within the muscles syncitium (Demontis and Perrimon, 2009). Also occurring during the larval stage is the active proliferation of *twist*-expressing cells. These cells form precursors of adult muscles (Bate et al.,

1991). The precursors for the adult head and thorax are stored in the larval imaginal discs and will contribute to the adult-specific muscle pattern during pupal development (Bate et al., 1991, Rivlin et al., 2000, and reviewed in Roy and VijayRaghavan, 1999).

The pattern of adult muscles bears little resemblance to the pattern of larval muscles. In order to form the adult muscles, at metamorphosis most larval muscles histolyze and adult muscles are formed *de novo* by migration and fusion of adult muscle precursor cells (Currie and Bate, 1991, Fernandes et al., 1991). Within these migrating populations, the new adult muscles develop in much the same manner as is observed for embryonic/larval muscles: founder cells are specified early during the pupal stage and myoblast fusion occurs, presumably through a mechanism similar to that defined for the embryo (Rivlin et al., 2000, Dutta et al., 2004, Atreya and Fernandes, 2008).

The nervous system plays a crucial role in the formation and patterning of adult muscles (Fernandes and Keshishian, 2004) but not in embryonic muscles (Broadie and Bate, 1993). Adult muscle development proceeds in parallel with neuronal restructuring during metamorphosis allowing one to interact with and influence the other (Fernandes and VijayRaghavan, 1993). In the absence of innervation, founder cell markers of the dorsal longitudinal muscles are lost around the time fusion would occur and the proliferation of myoblasts is reduced. It is unclear whether this occurs for other muscle types. Fusion of myoblasts is initiated when the developing neuron is denervated, however, muscle development cannot be sustained (reviewed in Roy and VijayRaghavan, 1999).

Adult muscles that develop *de novo* following histolysis of larval muscles are more sensitive to denervation than adult muscles formed by fusion of myoblasts to larval muscle scaffolds, such as the dorsal longitudinal muscles (Fernandes and Keshishian, 1998, Fernandes and Keshishian, 2004).

The final pattern of adult muscles is far more complex than that of the embryo (reviewed in Bernstein et al., 2003). While each individual embryonic muscle is composed of a single syncytial fiber, adult muscles are composed of multiple myofibers (reviewed in Baylies et al. 1998). The muscles of the embryo are arranged in a repeated segmental pattern with thirty muscles per hemisegment. By contrast, the adult musculature contains muscles that are larger and can span multiple segments. In addition to the differences in size and fiber number, the musculature of the *Drosophila* embryo and adult differ by the relative importance of innervation for proper muscle specification, the role of the epidermis in establishing muscle attachments and guiding myoblast migration to proper sites of development, and the role of hormone signaling in specifying the identity of the muscles (reviewed in Roy and VijayRaghavan, 1999). The adult fly is characterized by a vast diversity in muscle types, which differ from each other ultrastructurally, physiologically, and at the level of gene expression. Since each muscle of the adult fly has its own unique identity, in spite of undergoing a similar myogenic program to other muscles, it is important to study the mechanisms by which specific muscles are formed.

The study presented in Chapter 1 of this dissertation aims to further elucidate the mechanisms that are important for proper formation of the Tergal

Depressor of Trochanter (TDT or "jump") muscle in *Drosophila*. Specifically, the study aims to identify the gene that is affected by a mutation called *wings apart* (*wap*) that causes loss of the TDT. Both the genetic basis of the *wap* mutation and the phenotypic consequences of this mutation are explored. In addition, the mechanism by which the mutation causes loss of the TDT in adult flies is examined.

Chapter 2 focuses on the regulation of the *Mef2* gene in early mesodermal development. Although much is known about how this myogenic regulator is itself regulated, direct regulators at the earliest stages of development are yet to be fully characterized. This chapter assesses the potential combinatorial roles of the candidate transcription factors Twist and Mad on regulation of the early *Mef2* enhancer.

CHAPTER 1

IDENTIFICATION OF *CG14614* AS THE TRASCRIPTIONAL UNIT OF THE *WINGS APART* GENE IN *DROSOPHILA*

Abstract

The *wings apart* (*wap*, FBgn0004000) phenotype is due to a semi-lethal mutation located on the proximal X chromosome, mapped to region 20A. The *wap* mutation results in loss of the TDT. Prior to my study, it was unknown what transcription unit is mutated to produce the observed *wap* phenotype, nor which process of TDT development is affected by this mutation. In this study, complementation mapping and RNAi knockdown technology were used to identify *CG14614* (FBgn0031186) as the annotated gene model affected by the *wap* mutation. *CG14614* encodes a WD40 repeat protein homologous to the vertebrate *wdr68* gene found in skeletal muscle. Results of the RNAi knockdown also allowed for identification of *CG14619* (FBgn0031187) as the annotated gene model affected by the *intro* mutation. Analysis of TDT development in *wap* mutants indicated that TDT-specific founder cells are specified early in development but are later lost. The neuron that innervates the TDT reaches its target in *wap* mutants but neuromuscular junctions do not form properly. Insights from this study can help us elucidate mechanisms of neuromuscular development and facilitate understanding of neuromuscular diseases that may result from mis-expression of muscle-specific or neuron-specific genes.

Introduction

The degree to which many muscle diseases impact muscles often differs between distinct subsets of muscles, and some muscle diseases affect only specific muscle types (Tixier *et al*. 2010). Although as many as 25 genes have been implicated in congenital and degenerative muscle diseases, there remain some muscle diseases for which causative mutant genes are unidentified (Guyon

et al. 2007). It is well known that morphologically and functionally distinct subsets of muscles arise from a uniform pool of mesodermal cells and are regulated by similar genes and developmental mechanisms (Roy and VijayRaghavan, 1999). It is, therefore, important to understand how distinct muscle subsets are properly formed to better understand the genetic defects that lead to muscle diseases.

Muscle development is well conserved from insects to mammals (reviewed in Buckingham, 2006) and the basic structure of muscle fibers is also conserved from insects to mammals (Schulz *et al*., 1991). Furthermore, different subtypes of human muscle diseases are affected by mutations in genes with muscle specific-orthologs in *Drosophila* (Tixier, et al 2010). For these reasons, research using the model organism *Drosophila melanogaster* can provide insight into the basic mechanisms of muscle formation and patterning in more complex animals, such as vertebrates.

Two sets of muscles are formed during *Drosophila* development and serve different purposes throughout the fly life cycle. The embryonic musculature histolyzes at the onset of metamorphosis at which time the adult musculature is formed. The adult muscles are more complex and sophisticated than embryonic muscles (Fernandes et al., 2005) and more closely resemble those of vertebrate muscle systems (reviewed in Maqbool and Jagla, 2007). For example, adult muscles in *Drosophila* often are composed of multiple individual fibers; in addition, some adult muscles have been shown to require innervation for their normal development. The majority of information available regarding adult muscle development is based on studies of the thoracic musculature, including

the indirect flight muscles (IFMs) and the Tergal Depressor of Trochanter (TDT) (Roy and VijayRaghavan, 1999).

The TDT or “jump” muscle in adult Drosophila is necessary for the escape response (Nachtigall and Wilson, 1967) and is stimulated by excitation of the giant fiber system (Allen et al., 2000). During early metamorphosis, after histolysis of larval muscles, two populations of *twist*-expressing adepithelial myoblasts from the T2 leg imaginal disc migrate to the site of TDT myogenesis. The early developing TDT consists of 12-13 closely packed imaginal pioneer (IP or founder) cells (identified by elongated shape and large nuclei) surrounded by many small myoblasts (Rivlin et al., 2000). As fusion of founders and myoblasts proceeds, the TDT elongates dorsoventrally and makes contact with the epidermal cells on the dorsal side of the animal (Rivlin et al., 2000). At 24 hours after puparium formation (APF), the TDT appears as a group of fibers surrounding a core of mitotic myoblasts with unfused mitotic myoblasts located at the dorsal end (Rivlin et al., 2000).

The mature TDT spans the dorsoventral axis of the adult thoracic cavity (Miller, 1950) between the DVM I and DVM II muscles (Fernandes and VijayRaghavan, 1993) and attaches to the dorsal notum of the second leg tendon (Miller, 1950, referenced by Rivlin et al., 2000). It is innervated by the Posterior Dorsal Mesothoracic Nerve (PDMN), which is restructured from the larval Intersegmental Nerve (ISN) branching off of the ventral ganglion (Fernandes and VijayRaghavan, 1993).

The TDT is a tubular muscle comprised of 26-28 large and 4 small fibers organized into a rosette pattern, but can be drastically altered by defects in the genetic program specifying the TDT. Jaramillo et al. (Jaramillo et al. 2009) showed that components of the TGF-β signaling pathway are involved in regulating the specification of TDT-specific founder cells and subsequently the number of muscle fibers found in the mature TDT. Similarly, the vertebrate TGF-β molecule myostatin regulates fiber number. In addition to its role in the development of muscle fibers, the TGF-β pathway also influences multiple tissues in a context-dependent manner (reviewed in Kollias and McDermott, 2008).

The TGF-β signaling pathway is also required for proper wing morphogenesis (Khalsa *et al*., 1998) and signaling events are heightened within the presumptive wing crossveins (Ralston and Blair, 2005). Since components of the TGF-β signaling pathway have been shown to modulate developmental events in both the wing and TDT, mutations in crossvein patterning genes were examined to determine if these genes are components of the TGF-β pathway and if these genes play a role in specification of the TDT pattern (Cripps, unpublished data). One such mutant identified is *wings apart* (*wap*).

wap is a semi-lethal gene with mutant lethality occurring in the pupal stage, despite showing no delay in developmental timing (Schalet and Lefevre, 1973). *wap* escapers become entrapped in the food medium and die shortly after eclosion (Schalet and Lefevre, 1973). Escapers exhibiting the *wap* phenotype are characterized by wings slightly set apart, a darker than normal thorax, and one or

more additional crossveins between the second and third longitudinal veins of the adult wings (Schalet, 1972 and Schalet and Lefevre, 1973). Complementation mapping of polytene X chromosomes using *wap* alleles, induced by X-rays, chemicals, and p-element transpositions, indicate *wap* is localized to the 20A3-4 region of the X chromosome (Lifschytz and Falk, 1968, Lifschytz and Falk, 1969, and Eeken *et al.,* 1985). It is thought to most likely be between the *extra organs* (*eo*, FBgn0000580) and *uncoordinated-like* (*uncl*, FBgn0003951) loci, 20A2 and 20A5, respectively (Schalet, 1972). The exact location of the *wap* gene had not previously been definitively mapped to a single transcription unit due to difficulty in evaluating the proximal end of the X chromosome, most likely because of its strongly heterochromatic nature, and the large number of transposable elements in that region (Schalet and Lefevre, 1973, Eeken *et al*., 1985, and FlyBase FB2012_03). It is currently unknown what annotated gene model within this region is responsible for the phenotype associated with *wap* escapers.

In this study I show that the *wap* mutation not only affects the patterning of the wing crossveins but also causes a defect in TDT formation. Many of the *wap* mutant escapers completely lack the TDT while a very small percentage of these escapers exhibit a greater than 60% reduction in the number of muscle fibers. We also identify *CG14614*, a WD40 repeat protein, as the transcriptional unit that is mutated to cause the *wap* phenotype. In addition, we show that the founder cells that specify the TDT are present in the *wap* mutant early in development but are later lost leading to degeneration of the muscle. This degeneration is shown

to be due to defects in synaptogenesis at the neuromuscular junctions between the TDT muscle and the PDM nerve.

Materials and Methods

Drosophila stocks

Drosophila were grown on Carpenter's medium (Carpenter, 1950) at 25^{o}C unless otherwise specified. Fly stocks used in the X chromosome deficiency screening, mutation mapping crosses, Gal4 driver lines and X chromosome duplication screening were obtained from the Bloomington *Drosophila* Stock Center, with exception to those noted below. The stock carrying the *wap*^{3} allele was obtained from the *Drosophila* Genetic Resource Center, Kyoto Institute of Technology. The *Act79B*-Gal4 driver was made by Anton Bryantsev (unpublished). Mary Baylies (Memorial Sloan Kettering Cancer Center, NY) generously provided the *rP298-lacZ* transgenic line. UAS-RNAi lines were obtained from the Vienna Drosophila Stock Center (VDRC), except two UAS-*DIP1* RNAi lines obtained from the Transgenic RNAi Project (TRiP) at Harvard Medical School.

Deficiency screens

Each genetic cross was composed of equal numbers of virgin females and males and maintained at 25^{o}C. For deficiency screening with *wap* alleles, each mutant allele was crossed with the deficiency lines *Df(1)Exel6255* (Exelixis, Inc.), *Df(1)BSC708*, *Df(1)LB6*, *Df(1)54*, *Df(1)DCB1-35c*, *Df(1)DCB1-35b*, and *Df(1)R8A* (Schalet and Finnerty, 1968, Schalet and Lefevre, 1973 and Rahman and Lindsley, 1981). The number of progeny eclosed from each individual cross was

counted. Comparisons between the total numbers of female progeny with *balancer/mutation* genotype and female progeny with the *deficiency/mutation* genotype were performed using Student's t-test. Lethality of a combination was concluded only if crosses with each allele of the mutation resulted in lethality. Analyses of TDT and wing crossvein phenotypes were performed for both *balancer/wap* and *deficiency/wap* genotypes as described below.

The previously-mentioned deficiency lines were also crossed with each other to further refine the X chromosome map. These same deficiency lines were used to map other proximal X chromosome mutations thought to be within the region spanning 20A to 20C: *l(1)G0179*, $eo^{16\text{-}2\text{-}27}$, eo^{25}, $intro^{3}$, $uncl^{1}$, $uncl^{10}$, soz^{1}, $l(1)20Cb^{2}$, $l(1)20Cb^{6}$, $l(1)20Ca^{1}$, $l(1)20Ca^{2}$, and *l(1)G1096*.

Duplication screens

Virgin females of each mutation used in the deficiency screens were also crossed with equal numbers of males from X chromosome duplication lines spanning the region deleted by the *Df(1)Exel6255* deficiency. The duplication lines used in these experiments were *Dp(1;3)DC382*, *Dp(1;3)DC383*, *Dp(1;3)DC384*, *Dp(1;3)DC562*, *Dp(1;3)DC386*, *Dp(1;3)DC387*, *Dp(1;3)DC388*, *Dp(1;3)DC389*, and *Dp(1;3)DC390* (Popodi *et al*., 2010). Not all combinations of mutations and duplications were tested against one another since some mutations are complemented by deficiencies of the duplicated region. For those duplications tested, the number of eclosing male progeny with the genotype *balancer/Y;duplication/+* were compared with male progeny of the

mutation/Y;duplication/+ genotype using Student's t-test to assess the ability of each duplication tested to rescue the phenotype of the mutations.

To insure that any phenotypic rescue observed in the previous duplication analysis with *wap* was not due to rescue of a secondary mutation, lines were generated that had the genotype *Df(1)Exel6255/FM7a;duplication/duplication* and/or *Df(1)DCB1-35c/FM7a;duplication/duplication* for the each of the following duplications: *Dp(1,3)DC383*, *Dp(1,3)DC384*, *Dp(1,3)DC562*, *Dp(1,3)DC386*, *Dp(1,3)DC387*, *Dp(1,3)DC388*, *and Dp(1,3)DC389*. These lines were crossed with $wap^{2}/Dp(1,y)y^{+}mal^{171}$ males. Female $FM7a/wap^{2};duplication/+$ progeny were compared with female $deficiency/wap^{2};duplication/+$ progeny to assess whether the *wap* mutation can be rescued by the duplications. The TDT and wing crossvein phenotypes were assessed as described below for rescue by duplication.

RNAi knock-down

The Gal4/UAS system was utilized for RNAi knockdown experiments (Brand and Perrimon, 1993). Equal numbers of virgin female and male flies were allowed to mate three days at 25^{o}C at which point crosses were transferred to 29^{o}C to activate the Gal4 drivers. *tub*-Gal4 and *da*-Gal4 were used as ubiquitous drivers for initial RNAi analysis. To determine tissue specific effects of RNAi knockdown, *Act79B*-Gal4 and *1151*-Gal4 drivers were used for muscle-specific knockdown and *elav*-Gal4 was used for knockdown in the nervous system. UAS-RNAi lines were utilized for knockdown of *DIP1* (VDRC lines 50206, 50207, and 108186 and TRiP lines 35226 and 35333), *CG14614* (line 107076), *CG14619*

(lines 37929 and 37930), *CG14618* (lines 24879 and 47451), *CG12576* (lines 51205 and 104261), and *Cp110* (lines 24874, 24875, and 101161). RNAi knockdowns were assessed for viability. TDT formation was assessed by cryosections of pharate pupae of the pupal lethal knockdowns as described in the following sections.

Recombination experiment

To obtain flies carrying both the wap mutation and the founder cell-specific *rP298-lacZ* transgene (described in Ruiz-Gomez *et al*., 2000), I performed recombination crosses. Female *FM7i,GFP/wap* mutants were crossed with equal numbers of rP298-*lacZ* transgenic males. Both the wap^{2} and wap^{9} alleles were used for these crosses. rP298-*lacZ*/*wap* female progeny from the F_1 generation were selected as virgins and crossed with *FM7i,GFP/Y* males. Each female of the F_2 generation was isolated individually as virgins and again crossed with *FM7i,GFP/Y* males to establish stable stocks.

Progeny from these crosses were assessed for presence of the wap mutation by observing the Bar-eye phenotype associated with the FM7i, GFP balancer. The presence of males with wild-type eye morphology indicated that the lethal *wap* mutation could not be present in the generated stock. To screen for the presence of the rP289-*lacZ* transgenic marker, two adult flies from each line positive for the *wap* mutation were filleted and stained overnight at 37^{o}C in XGAL solution [1X PBS, 100 mM $K_4[Fe(CN)_6]$, 100 mM $K_3[Fe(CN)_6]$, 150 mM NaCl, 1 mM $MgCl_2$, and 0.2% w/v X-Gal (Sigma)]. Stocks positive for both the

wap mutation and rP298-*lacZ* transgene were used in pupal dissections described below.

Preparation of samples for microscopy

Samples to be analyzed for TDT structure were prepared for paraffin sectioning according to methods described by Lyons *et al*. (Lyons *et al*., 1990), modified by Cripps *et al*. (Cripps et al. 1998). Sections were cut at 10 µm and stained with Hematoxylin and Eosin (Sigma). Stained slides were dehydrated through 100% ethanol, soaked in xylene, and mounted in Cytoseal-XYL (VWR Scientific products).

Cryosections were prepared by removing pharate pupae from the pupal case, embedding in OTC medium and freezing. Sections were cut at 10 µm at -18^{o}C and air dried. Samples were fixed for 8 minutes at room temperature with 3.7% v/v formaldehyde in PBTx [1XPBS, 0.2% v/v Triton-X100, 0.2% w/v Blocking Agent (Roche)], washed and used for antibody staining as described in the following section.

For pupal dissections to assess founder cell specification and neuromuscular junction formation, new white prepupae were selected and aged until the appropriate time for dissection. Pupal samples were dissected in a Sylgard-coated petri dish (Dow Corning) and pinned open. Samples were fixed for 30 min on ice in 5% formaldehyde in 1X PBS, washed in PBTx, then subjected to blocking and incubated with antibody (described below).

For analysis of the crossveins of the adult wings, wings were removed from adult flies and stored overnight in 70% (v/v) ethanol. Wings were transferred

twice into 100% ethanol and soaked in 100% xylene prior to being mounted in Cytoseal-XYL (VWR Scientific Products) for imaging.

Immunohistochemistry of prepared samples and imaging

Fixed and washed samples were stained with antibodies as described by Patel (Patel, 1994) and modified by Molina and Cripps (Molina and Cripps, 2001). Primary antibodies used for cryosections were anti-βPS-integrin 1:10 (Brower *et al*., 2008) (University of Iowa Developmental Studies Hybridoma Bank). For pupal dissections, primary antibodies used were mouse anti-β-galactosidase 1:400 (Promega), rabbit anti-MEF2 1:1000 (Lilly *et al*., 1995) (provided by Bruce Paterson, NIH), mouse anti-22C10 1:100 (University of Iowa Developmental Studies Hybridoma Bank), rabbit anti-HRP 1:25 (GenScript), and mouse anti-Dlg 1:10 (University of Iowa Developmental Studies Hybridoma Bank). For immunofluorescence of sections, Alexa conjugated (Molecular Probes) secondary antibodies were mixed with Alexa-488 phalloidin at 1:500 (Molecular Probes) and 2 µg/mL DAPI (Sigma). Alexa-conjugated secondary antibodies were diluted to 1:2000 for pupal stains.

An Olympus BX-51 stereomicroscope with DIC or fluorescent optics was used to collect images. Adobe Photoshop was used to compile digitally collected images into figures.

Results

wings apart (*wap*) mutants are characterized by three phenotypes

Mutants with defects in the crossveins of the adult wings were examined to determine if these mutants also exhibit TDT defects since components of

signaling pathways involved in wing vein development are also involved in proper TDT development. Mutant thoraces were visualized in paraffin sections cut horizontally to the muscle axis (unpublished data). One of the mutants analyzed was the *wings apart* (*wap*) mutant that is characterized by three phenotypes (Figure 1). Figure 1A shows the wing of an adult wild-type fly. In a wild-type wing, there are five longitudinal veins and two crossveins. By contrast, the *wings apart* mutant has supernumerary crossveins located between the second and third longitudinal veins (arrows in Figure 1B). The TDT of the wild-type fly is organized in a rosette pattern, between the DVM I and DVM II muscles (Figure 1C). When paraffin sections of the thoracic muscles were visualized in the *wap* mutant, we observed that the TDT is absent while no other thoracic muscles are affected (asterisk in Figure 1D). In addition to the wing and TDT phenotypes, *wap* mutants are semi-lethal as homozygotes (Schalet, 1972) and this semi-lethal phenotype is observed in heteroallelic combinations of three *wap* alleles (Figure 1E). Since the phenotypes are observed in all homozygous lines of *wap* mutants, as well as in heteroallelic combinations of the alleles, we can conclude that the phenotypes all arise from the same mutation.

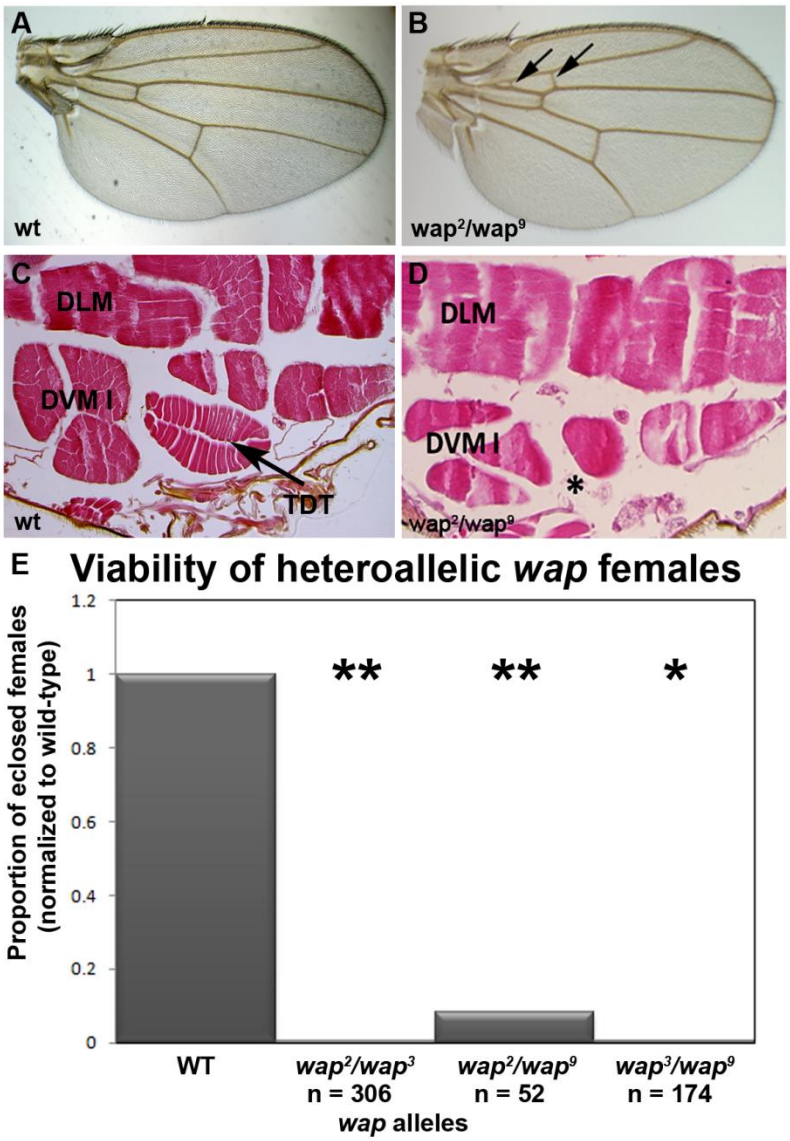

Figure 1: The *wings apart* (*wap*) mutation is characterized by three phenotypes. (A, B) Wings from *wap* escapers (B) have additional crossveins (arrows) between the second and third longitudinal veins compared with wild-type wings (A). (C, D) The TDT in wild-type flies is located between the DVM I and DVM II (C). The TDT is absent in *wap* mutants (asterisk in D). (E) Compared to wild-type flies, *wap* heteroallelic mutants exhibit a semi-lethal phenotype, similar to that of *wap* homozygous mutants. (*p<0.01, **p<0.001)

wap is located in region 20C in the proximal X chromosome

Mapping of the *wap* mutations by Lifschytz and Falk suggested that *wap* is located on the proximal X chromosome in region 20A3-4 (Lifschytz and Falk, 1968, grey highlighted region in Figure 2). To more precisely localize the

transcriptional unit affected by the *wap* mutation, each of the *wap* mutant alleles was crossed with the deficiency lines *Df(1)Exel6255* (Exelixis Inc.), *Df(1)BSC708*, *Df(1)LB6*, *Df(1)54*, *Df(1)DCB1-35c*, *Df(1)DCB1-35b*, and *Df(1)R8A* (Schalet and Finnerty, 1968, Schalet and Lefevre, 1973 and Rahman and Lindsley, 1981).

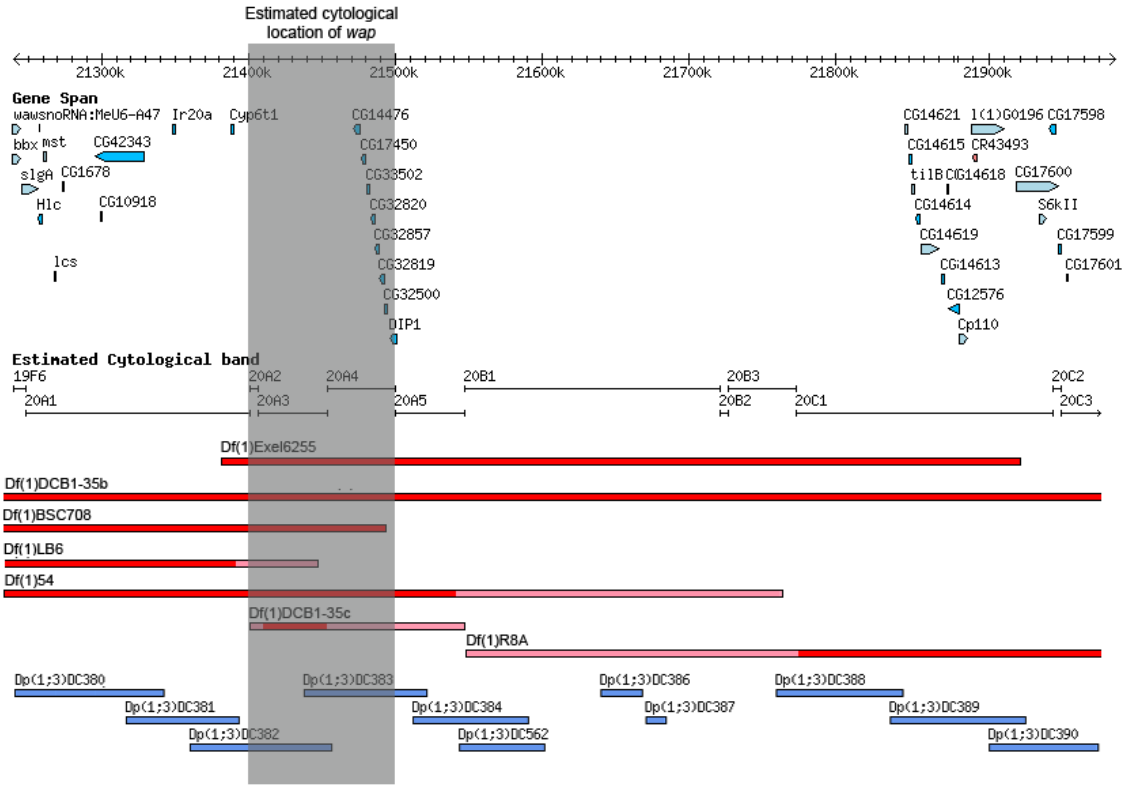

Figure 2: *wap* was previously mapped to region 20A2-3 of the proximal X chromosome. The map of the proximal X chromosome indicates annotated genes (light blue bars) located between 19F6 and 20C1 of the X chromosome. The deficiencies used in this study are shown on the map by the red bars. Deficiencies Df(1)Exel6255 and Df(1)BSC708 are molecularly mapped. Other deficiencies were added to the map based on computed cytological location, but have undefined breakpoints (denoted by pink bars). Lower blue bars indicate the positions of molecularly defined duplication lines used in this study. The grey highlighted region denotes the region where *wap* was initially mapped. (Image was adapted from the map on FlyBase (FB2012_02).)

Results from complementation mapping of *wap* alleles with the deficiency lines indicated in Figure 2 (red bars) indicate that the deficiency lines *Df(1)BSC708*, *Df(1)LB6*, and *Df(1)R8A* complement *wap*. The data in Figure 3A

represent aggregate results for the *wap*^{2} and *wap*^{9} alleles. The *wap*^{3} allele was not included in the aggregated results but exhibited significantly reduced viability with the Df(1)BSC708 and Df(1)R8A deficiencies (data not shown). These two deficiencies nevertheless complemented *wap*, since *wap*^{2} and *wap*^{9} show strong viability in trans to the deletions. It is likely that the *wap*^{3} chromosome contains a second lethal mutation on it that is uncovered by *Df(1)BSC708*. The lethality observed for the *Df(1)R8A* deficiency with *wap*^{3} was due to the presence of the *Df(1)R36* (Rahman and Lindsley, 1981) deletion on the same chromosome as the *wap*^{3} allele. If data from the *wap*^{3} allele is included in the analyses of these deficiencies, the percentage of eclosed females heterozygous for *wap* and the Df(1) BSC708 and Df(1)R8A deficiencies decreases to 63.5% and 52.3%, respectively, while these data for the other complementation analyses remain unaffected (data not shown).

There are also four deletion lines, *Df(1)Exel6255*, *Df(1)54*, *Df(1)DCB1-35c*, and *Df(1)DCB1-35b*, that are semi-lethal when heterozygous with the *wap* mutant (Figure 3A). These data suggest the region proximal to the *Df(1)BSC708* deletion and distal to the *Df(1)R8A* deletion is the region in which *wap* is located. To confirm that these escapers show all three *wap* phenotypes, the wings and thoraces of females heterozygous for the deficiencies and *wap* were analyzed by for the presence of the wing and TDT phenotype characteristic of *wap*. Those heterozygous females from the deficiency lines that complemented wap had normal wings and the TDT was present (Figure B and C, results from *Df(1)BSC708/wap*^{2} shown). The escapers from the semi-lethal heterozygotes

exhibited an additional crossvein between the second and third longitudinal vein, characteristic of *wap* homozygous mutants (Figure 3D). The TDT in almost all of these heterozygous females was completely absent (Figure 3E, results from *Df(1)Exel6255/wap*^{2}). It is important to note that although almost all escapers lack the TDT muscle, a small percentage of the escapers, 3% (n=64), had a TDT; however, the muscle exhibited abnormal morphology and a greater than 60% reduction in the number of fibers compared with a wild-type TDT muscle (10 to 12 fibers in mutants compared with 30-32 fibers in wild-type).

Results of these analyses and previously published work (Lifschytz and Falk, 1968) suggest that a likely candidate for the *wap* phenotype is *DIP1,* as it is the only gene deleted by all four deficiencies located in region 20A, as long as we assume that the polytene band annotations to the genome are accurate. We sought to confirm this result using molecular analysis by sequencing the entire *DIP1* gene in both the *wap*^{2} and *wap*^{9} alleles. We observed no non-synonymous amino acid substitutions within the coding region of the *wap*^{2} allele relative to the *Drosophila melanogaster* reference sequence (FB2012_03) and only a single variation within the coding region of the *wap*^{9} allele (data not shown). It remained unclear whether this mutation observed in the *wap*^{9} allele was significant to the function of *DIP1* or if it was alternatively due to variation in the *DIP1* gene among individual flies. Additionally, we were unable to reproduce the *wap* phenotypes by RNAi knockdown of *DIP1* when using a number of different RNAi lines, and different Gal4 drivers (data not shown).

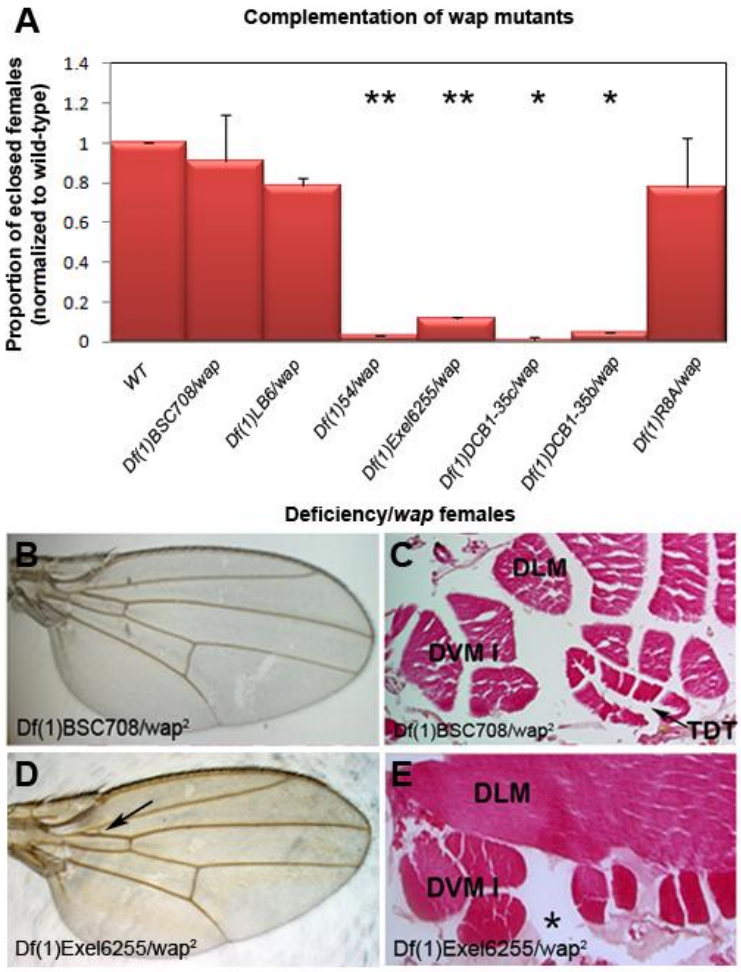

Figure 3: *wap* mutations are lethal when heterozygous with four of the tested deficiencies. (A) Proportion of eclosed females heterozygous for wap and the indicated deficiencies. Lethality was observed when wap was heterozygous with Df(1)54 (n = 104), Df(1)Exel6255 (n = 508), Df(1)DCB1-35c (n = 275), and Df(1)DCB1-35b (n = 114). (*p<0.01, **p<0.001) Df(1)BSC708 (n = 774), Df(1)LB6 (n = 304), and Df(1) R8A (n = 564) complemented *wap*. (B, C) Wings and thoraces of wap flies heterozygous with complementing deficiencies resemble the wild-type phenotype. (D, E) Wings and thoraces of mutants heterozygous for lethal deficiencies recapitulated the phenotype observed for wap homozygous mutants. The presence of an additional crossvein (arrow in D) was observed for with the lethal deficiencies. These deficiencies also resulted in loss of the TDT (asterisk in E) when heterozygous with wap.

Due to inconsistencies between the initial deficiency mapping of *wap* and the molecular analysis of *DIP1*, we sought to refine our mapping by performing complementation tests of the deficiencies themselves. This was done based on the possibility that annotated, computed breakpoints obtained from the FlyBase

database (FB2012_02) for several of the deficiencies (*Df(1)LB6*, *Df(1)54*, *Df(1)DCB1-35c*, *Df(1)DCB1-35b*, and *Df(1)R8A*) may not be located within the predicted region (indicated by the map in Figure 2). In this scenario, those genes located in region 20C1 and that are deleted by *Df(1)Exel6255* cannot be ruled out as candidates for *wap*. Results found in Table 1 demonstrate complementation of *Df(1)BSC708* and *Df(1)LB6* with *Df(1)DCB1-35c*, suggesting that the proximal breakpoints for both *Df(1)BSC708* and *Df(1)LB6* are to the left (i.e., centromere distal) of the distal breakpoint for *Df(1)DCB1-35c*. The proximal breakpoints for *Df(1)54* and *Df(1)DCB1-35c* are left of the distal breakpoint for *Df(1)R8A*, as both of these are complemented by the *Df(1)R8A* deficiency (Table 1, last column). The distal breakpoint of *Df(1)R8A* is also more proximal than the proximal breakpoint of *Df(1)Exel6255* as inferred from complementation between these two deficiencies. The Df(1)DCB1-35b deficiency spans the entire region tested, as previously reported (Schalet and Finnerty, 1968) and does not complement Df(1)R8A.

	Deficiency mapped						
Deficiency/Deficiency	*Df(1)BSC708*	*Df(1)LB6*	*Df(1)54*	*Df(1)Exel6255*	*Df(1)DCB1-35c*	*Df(1)DCB1-35b*	*Df(1)R8A*
Df(1)BSC708	-	-	-	-	-	-	+
Df(1)LB6		-	-	-	+	-	+
Df(1)54			-	-	-	-	+
Df(1)Exel6255				-	-	-	+
Df(1)DCB1-35c					-	-	+
Df(1)DCB1-35b						-	-
Df(1)R8A							-

Table 1: Viability of deficiencies mapped to the other deficiencies.
NT indicates the deficiency lines were not crossed.
+ indicates complementation of the deficiencies,
- indicates lethality.

While the mapping of the deficiencies resolved some of the inconsistencies in the locations of deficiency breakpoints, it was still not adequate to completely refine the map of this genetic region. I therefore complementation mapped additional mutations previously known to be located within the same region of the proximal X chromosome, for which the corresponding transcriptional units have yet to be identified from among the annotated gene models. These mutations are thought to affect predominantly single genes rather than multiple genes. If the mapping has sufficient resolution, candidate genes for the different mutants could be inferred (Table 2, mutants arranged according the predicted order on the chromosome).

The *mutant/deficiency* complementation data suggested that the locations of the mutations, relative to each of the other mutations tested, remain in the original map order, with the exception of *l(1)20Ca* and *l(1)20Cb*, for which the order was switched. However, the regions to which each of these mutations are located on the chromosome map does change.

The results presented in Table 2 indicate that the mutant *l(1)G0179* is deleted by both *Df(1)LB6* and *Df(1)54*, but not by the other deletions. *l(1)G0179* is complemented by *Df(1)BSC708* suggesting its actual location on the chromosome is distal to region 19E7, where the breakpoint of *Df(1)BSC708* is located (based upon annotation of cytological regions relative to annotated genomic coordinates on FlyBase, FB2012_02). It also suggests that the distal breakpoint of *Df(1)54* extends even further distal to its computed breakpoint of

19F1 and the mapped breakpoint of Df(1)BSC708, although the exact extent of the deletion remains unknown.

Table 2 also indicated that the lethal *extra organs* (*eo*, FBgn0000580) mutation lies between the *Df(1)BSC708* and *Df(1)DCB1-35c* deficiencies but is not complemented by *Df(1)LB6*, suggesting that the proximal breakpoint for the *Df(1)LB6* deficiency is to the right of the proximal breakpoint for *Df(1)BSC708*.

The complementation results for the *introverted* (*intro*, FBgn0001268) mutation were very similar to those obtained for the *wap* mutation (Table 2 and Figure 3A). For both of these mutants, the mutation was localized to the region between the proximal breakpoint of *Df(1)LB6* and the between the proximal and distal breakpoints of *Df(1)DCB1-35c*.

The *uncoordinated-like* (*uncl*, FBgn0003951) mutant was complemented by all the deficiencies except *Df(1)54* and *Df(1)DCB1-35b*. This suggests that the mutation lies proximal to *Df(1)Exel6255* and distal to *Df(1)R8A*. What is also suggested by these results is that one breakpoint of the *Df(1)54* deficiency must also be found within the region between the breakpoints of these deficiencies. It is important to note that results were not consistent between the two *uncl* alleles used for the mapping (denoted by the asterisk in Table 2). A condition for lethality in this analysis is that the deficiency tested must fail to complement all alleles tested for a specific mutant. The analysis of these mutant alleles indicated that the $uncl^{1}$ allele was lethal with all deficiencies except *Df(1)LB6*, suggesting that additional mutations may be present in the proximal region of the X chromosome in $uncl^{1}$ mutants.

Both the *sozzled* (*soz*, FBgn0001568) and *l(1)20Ca* (FBgn0001569) mutants were complemented by all the deficiencies except *Df(1)DCB1-35c*. This indicates that the location of these two mutations lies between the breakpoints of *Df(1)Exel6255* and *Df(1)R8A* and proximal to *uncl* and the proximal breakpoint of *Df(1)54*. Lastly, the *l(1)20Cb* (FBgn0001570) mutant is complemented by all deficiencies, except for *Df(1)R8A*.

	Mutation mapped							
Deficiency/mut	l(1)G0179	eo	intro	wap	uncl	soz	l(1)20Cb	l(1)20Ca
Df(1)BSC708	+	+	+	+	-	+	+	+
Df(1)LB6	-	-	+	+	+	+	+	+
Df(1)54	-	-	-	-	-	+	+	+
Df(1)Exel6255	+	-	-	-	-	+	+	+
Df(1)DCB1-35c	+	+	-	-	+	+	+	+
Df(1)DCB1-35b	NT	-	-	-	-	-	+	-
Df(1)R8A	+	+	+	+	+	+	-	+

Table 2: Viability of mutations mapped by deficiencies.
Two alleles of each mutation, except *l(1)G0179*, *intro*, and *soz*, were crossed to each deficiency.
NT indicates the mutation was not tested with the deficiency.
*Two alleles of *uncl* were tested with inconsistent results between the alleles.

To provide additional rigor to the deletion mapping data, each mutation tested in the above experiments was subjected to complementation experiments using duplication lines (blue bars in Figure 2) to rescue the phenotype observed in the mutants (Table 3). The duplication lines selected were those that span the region deleted by the *Df(1)Exel6255* deficiency, since this deletion failed to complement *wap*; moreover, the breakpoints of this deficiency have been molecularly mapped. Not all of the duplications were tested with all the mutations, since the deficiency analysis suggested some mutations cannot be located in the regions duplicated. The analysis showed that, consistent with our deficiency screen data, the *l(1)G0179*, *l(1)20Cb*, and *l(1)20Ca* mutations cannot be rescued by any of the duplication constructs tested.

The *eo* mutation also could not be rescued by any of the tested duplications. This could be due to the presence of more than one lethal mutation on the *eo* mutant chromosome or perhaps, the entire region required for expression of the *eo* gene product or some key regulatory region is not duplicated by the duplication line being tested. It is not surprising that the *uncl* mutation cannot be rescued by any of the duplications since the results from the deficiency screen suggested that multiple sites on the X chromosome were affected by the *uncl* mutation. *soz* was rescued by the *Dp(1;3)DC390* duplication, refining the location of this gene to the region mapped in the complementation analysis.

	Mutation mapped								
Duplication/mutation	*l(1)G0179*	*eo*	*intro*	*wap*	*Deficiency/wap*	*uncl*	*soz*	*l(1)20Cb*	*l(1)20Ca*
Dp(1;3)DC382	-	-	NT	-	NT	-	-	NT	NT
Dp(1;3)DC383	-	-	NT	-	-	-	-	NT	NT
Dp(1;3)DC384	-	-	NT	-	NT	-	-	NT	NT
Dp(1;3)DC562	NT	-	-	-	-	-	-	NT	NT
Dp(1;3)DC386	NT	-	-	-	-	-	-	NT	NT
Dp(1;3)DC387	NT	-	-	-	-	-	-	NT	NT
Dp(1;3)DC388	NT	-	-	-	-	-	-	-	-
Dp(1;3)DC389	NT	-	+	+	+	-	-	-	-
Dp(1;3)DC390	NT	NT	-	-	NT	-	+	-	-

Table 3: Rescue of mutations by X chromosome duplications.
intro and *wap* are rescued by *Dp(1;3)DC389*.
soz is rescued by *Dp(1;3)DC390*.
NT indicates the mutation was not tested with the duplication.

Data presented in Table 3 also indicate the ability of *Dp(1;3)DC389* to rescue both *intro* and *wap*. This alone suggests that *intro* and *wap* are both located in the 92,593 bp region duplicated by *Dp(1;3)DC389*. Thus, *DIP1* cannot be the gene responsible for *wap*, as the deficiency analysis previously suggested. When we crossed lines of D*f(1)Exel6255/FM7a; Dp(1;3)DC389/Dp(1;3)DC389* with $wap^{2}/Dp(1,Y)y^{+}mal^{171}$ males, we were able to rescue $Df(1)Exel6255/wap^{2}$ females that were lethal in the absence of the duplication (Figure 4A). We were also able to rescue $Df(1)DCB1\text{-}35c/wap^{2}$ females with the *Dp(1;3)DC389* duplication using the same approach; however, this result is less significant considering that the *Df(1)DCB1-35c* deficiency can itself be fully rescued by the *Dp(1;3)DC389* duplication (data not shown). Thoraces from the both $Df(1)Exel6255/wap^{2};Dp(1;3)DC389/+$ females and $Df(1)DCB1\text{-}35c/wap^{2};Dp(1;3)DC389/+$ female have a wild-type wing phenotype (Figure 5B, see Figure 1A for comparison) and have a fully formed TDT (Figure 5C, see Figure 1C). A few escapers eclosed from the lines with the *Dp(1;3)DC383*, *Dp(1;3)DC386*, and *Dp(1;3)DC388* duplications. These flies were not considered to be rescued by these duplications as all escapers died shortly after eclosion, had extra wing veins, and lacked the TDT muscles (data not shown).

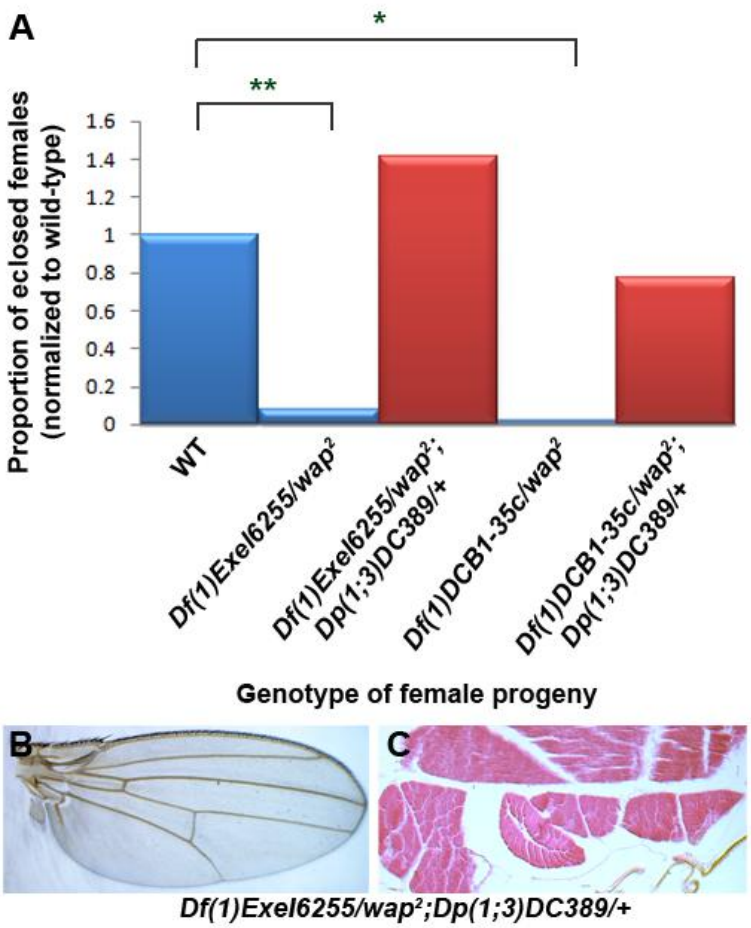

Figure 4: *Dp(1;3)DC389* rescues *Df(1)Exel6255/wap^2* and *Df(1)DCB1-35c/wap^2* heterozygotes. (A) Df(1)Exel6255/wap^2 (n = 410) and Df(1)DCB1-35c/wap^2 (n = 234) are lethal but can be rescued by Dp(1;3)DC389 (n = 53 and n = 108, respectively). (*p<0.01, **p<0.001) (B, C) Df(1)Exel6255/wap2;Dp(1;3)DC389/+ females have wild-type phenotypes.

Based on the above information, it is necessary to draw a new map of region 20A to 20C. Figure 5 incorporates all the data obtained from this study into a new map presenting a clearer picture of the *wap* location. The map presented extends the region deleted in *Df(1)LB6* beyond the proximal breakpoint of *Df(1)BSC708*. Although it remains unclear where the proximal breakpoint of *Df(1)LB6* is located (pink bars in Figure 5), it cannot extend beyond the *touch insensitive larva B* (*tilB*, FBgn0014395) gene as this deficiency can complement *tilB* mutations (Kavlie *et al.* 2010).

The region deleted by the *Df(1)54* deficiency can also be extended such that the map reflects the proximal breakpoint of this deletion being located between the proximal breakpoint of *Df(1)Exel6255* and the distal breakpoint of *Df(1)R8A* and within the region duplicated by *Dp(1;3)DC390*, but cannot definitively say where this breakpoint is located. As is the case with the proximal breakpoints of *Df(1)LB6* and *Df(1)54*, the position of the distal breakpoint of *Df(1)R8A* cannot accurately be defined. However, it is clear from the data that this deletion does not overlap with any of the other deficiencies used in this screen except for *Df(1)DCB1-35b*. It was also established that the entire deletion in the *Df(1)DCB1-35c* deficiency line is located in the region where the *Dp(1;3)DC389* is located. The location of the distal breakpoint can also be restricted to the region proximal to *tilB* since this gene is complemented by *Df(1)DCB1-35c* (Kavlie *et al*. 2010). The regions where the *eo*, *wap*, *intro*, *uncl*, *soz*, and *l(1)20Ca* mutations are most likely found can be added to this map.

eo is located within the region between the proximal breakpoint of *Df(1)BSC708* and *tilB*, in which there are three genes—*DIP1*, *CG14621*, and *CG14615*. The key to identifying what transcriptional unit is affected by this mutant is to determine the precise molecular coordinates of the *Df(1)LB6* proximal breakpoint. *uncl*, *soz*, and *l(1)20Ca* are located proximal to *Dp(1;3)DC389* but further analysis is required to define their precise locations.

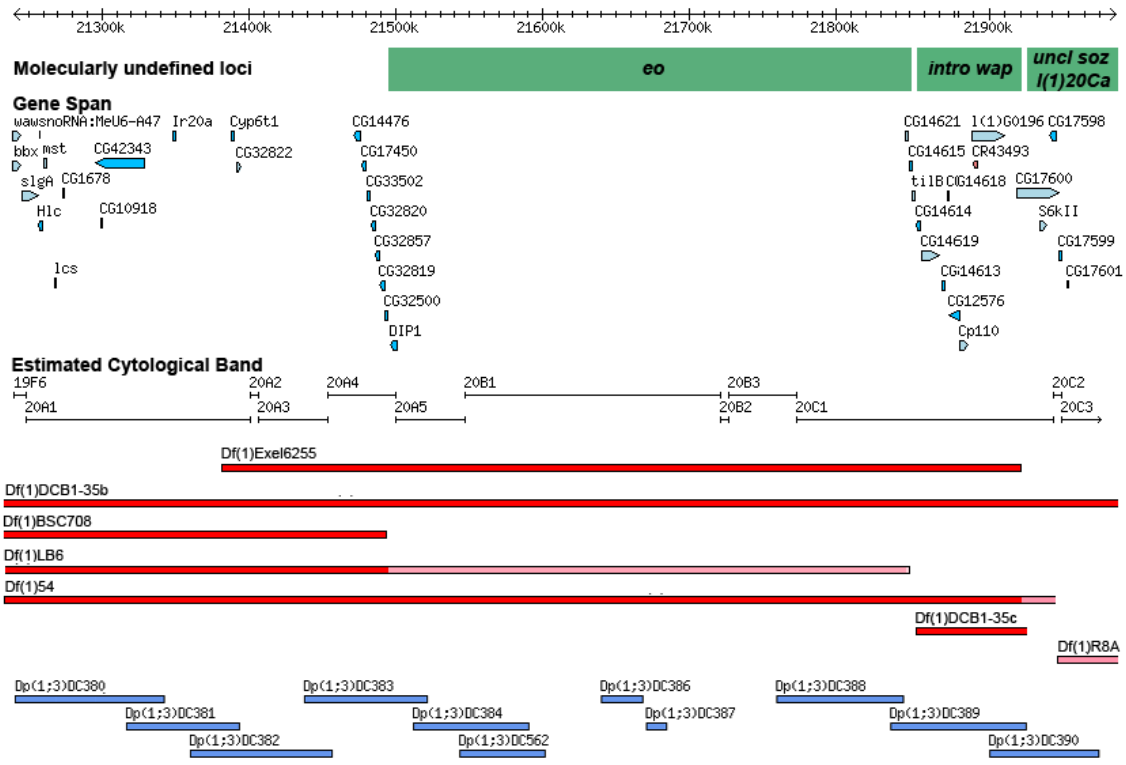

Figure 5: Refined map of the proximal X chromosome. The map from Figure 2 was redrawn based on the results of mapping experiments. Positions of breakpoints for Df(1)LB6, Df(1)54, Df(1)DCB1-35c, and Df(1)R8A were adjusted but are still not molecularly defined. Undefined breakpoint are represented by pink bars. Green bars indicate the region where mutations must be located.

CG14614 is the gene responsible for the *wap* phenotype

Both *wap* and *intro* are found within the region defined by *Df(1)DCB1-35c* and *Dp(1;3)DC389*. Six genes, *CG14614* (FBgn0031186), *CG14619* (FBgn0031187), *CG14613* (FBgn0031188), *CG14618* (FBgn0031189), *CG12576* (FBgn0031190), *Cp110* (FBgn0031191), and *l(1)G1096* (FBgn0027279), are found in this region. *wap* was complemented by a *l(1)G0196* mutant suggesting *l(1)G0196* is not the gene responsible for the *wap* phenotype (data not shown). For the other genes in the region, RNAi was performed to knock down expression of the products encoded by each gene using the well-established *Drosophila* Gal4/UAS system (Brand and Perrimon, 1993). The rationale for this

experiment was that by individually knocking down expression of each of the remaining candidate genes, it should be possible to recapitulate the *wap* phenotypes when the correct gene is knocked down. I initially carried out the knockdowns using the constitutively expressed Gal4 lines *tub*-Gal4 and *da*-Gal4.

Table 4 lists the genes in the region for which RNAi constructs were available, along with the results of the knockdown with both the *tub*-Gal4 (Lee and Luo, 1999) and *da*-Gal4 (Dura, 2005.12.4) drivers. Knock down of *CG14613* was not tested due to unavailability of an RNAi construct. No lethality was observed in a *CG14618* knock down and the knock down flies had a normal TDT. This gene was therefore ruled out as a candidate for *wap*. Viability was also observed when *da*-Gal4 was used to knock down *CG14619* (line 37929), *CG12576* (line 51205), and *Cp110* (all lines). Lethality was observed when *da*-Gal4 was used to drive knock down of *CG14614* and *CG14619* (line 37930). The *tub*-Gal4 driver was able to cause lethality when used to knock down *CG14614*, *CG14619* (both lines), *CG12576* (line 104261), and *Cp110* (line 101161). All but one (*CG12576*) of the lethal *tub*-Gal4 knockdowns were lethal in the pupal stage. We were able to rule out *CG12576* as a candidate for *wap* since *wap* mutants survive until the pupal stage. This left *CG14614*, *CG14619*, *CG14613*, and *Cp110* as candidates for the gene responsible for the *wap* phenotype.

Gene targeted	VDRC Line number	Off targets	*tub*-Gal4 driver phenotype	*da*-Gal4 driver phenotype
CG14614	107076	0	pupal lethal, reduced or absent TDT	lethal 2 days post eclosion, reduced or absent TDT
CG14619	37929	23	pupal lethal, failure of head eversion	viable, normal TDT
	37930	23	pupal lethal, failure of head eversion	pupal lethal, failure of head eversion
CG14618	24879	0	viable	viable, normal TDT
	47451	0	viable	viable, normal TDT
CG12576	51205	1	viable	viable, normal TDT
	104261	0	larval lethal	NT
Cp110	24874	0	viable	viable, normal TDT
	24875	0	viable	viable, normal TDT
	101161	0	pupal lethal, normal TDT	viable, normal TDT

Table 4: Genes knocked down by RNAi.
UAS-RNAi lines for the indicated genes were obtained from VDRC stock center.
Genes were tested using both the *tub*-Gal4 and *da*-Gal4 drivers.

I next wanted to determine if I had reproduced the *wap* TDT phenotype with any of the knock down experiments for the remaining candidates. Since *CG14614*, *CG14619*, and *Cp110* are all lethal in the pupal stage, pharate pupae were removed from their pupal cases and cryogenically sectioned to assess the TDT morphology. Figure 6A is an example of the adult thoracic musculature. The TDT is positioned on the lateral side of the thorax, between DVMs I and II. The TDTs of *Cp110* and *CG14619* knockdown flies developed normally compared with the wild type flies (Figure 6B and C, arrows). Based on this observation, both *Cp110* and *CG14619* can be ruled out as candidates for *wap*. RNAi knock down of *CG14614* resulted in flies that had absent TDT muscles (asterisk in Figure 6D) or reduced TDT fiber number (arrows in Figures 6E and 6F). In these knock downs, like the *wap* mutants, the majority of the flies analyzed were missing their TDTs with a few exhibiting a fifty percent or greater reduction in the number of TDT fibers. There were also some flies that exhibited both phenotypes, with a reduced phenotype TDT on one side of the thorax and one missing TDT on the contralateral side. These results strongly suggest that the gene that is mutated to give rise to the *wap* phenotype is *CG14614*.

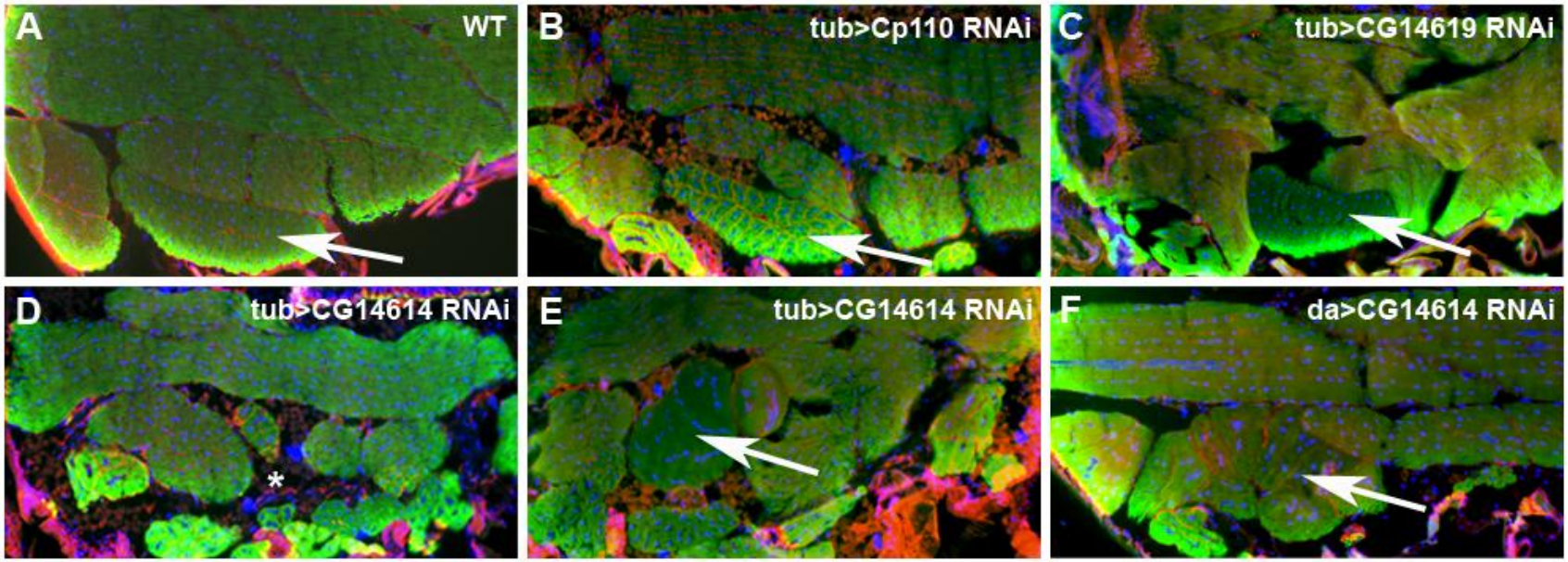

Figure 6: Knock down of *CG14614* reproduces the TDT phenotype observed in wap mutants. Pharate pupae from RNAi experiments resulting in pupal semi-lethal phenotype were sectioned cryogenically and stained with phalloidin (green) to label the muscles, βPS-integrin (red) to visualize membranes, and DAPI (blue) to label nuclei. (A) The TDT (arrow) is positioned between DVM I and DVM II. (C, D) Knock down of *Cp110* and *CG14619* with *tub*-Gal4 did not affect TDT formation. The indirect flight muscles in (C) are clearly affected by the knock down but the observed disorganization is presumably due to the presence of head structures in the thorax. (D-F) Knock down of *CG14614* with *tub*-Gal4 and *da*-Gal4 resulted in TDT absence (asterisk in D) or reduced number of TDT fibers (E, F).

CG14619 is a likely candidate gene mutated in *intro* mutants

CG14619 was ruled out as a candidate for *wap* based on the presence of a normally developed TDT. However, prior to sectioning, there was noticeable difference in the pupae of these knock downs (Figure 7). While wild-type flies had three obvious body segments and fully elongated wings and legs (bracket in A') located in the middle region of the pupa (Figure 7A-7A''), the knock down of *CG14619* resulted in the presence of only two developed body segments, the thorax and abdomen, and failure of head eversion (Figure 7B-7B''). The phenotype was even more obvious when the pupa was removed from the pupal case (Figure 7B''' compared with wild-type in Figure 7A'''). This phenotype is reminiscent of the described pupal phenotype of *intro* mutants (described as mutation 23 by Lifschytz and Falk, 1969). In addition to the failure of head eversion, the wing and leg discs in these knockdowns did not fully elongate and were located at the top of the pupal case where the thorax is located (brackets in B').

Since there are a number of off-targets associated with the RNAi lines used for the *CG14619* analysis (see Table 4), I wanted to confirm that my results were due to knock down of *CG14619* and not due to effects of off-target knock down. Our earlier mapping data suggested that the *intro* mutation is found within the 20C1 region we analyzed by RNAi. As the phenotype observed for *CG14619* knockdown were similar to the *intro* phenotype described by Lifschytz and Falk (1969), we also analyzed the pharate pupal phenotype of *intro* homozygous mutants. When the *CG14619* knock downs were compared with *intro* mutants,

both exhibited the same failure of head eversion and wing and leg elongation (Figure 7C-7C’’’). These results indicate that *CG14619* is the most likely candidate gene affected by the *intro* mutation.

In summary for the genetic mapping analysis, I have demonstrated that the *wap* gene is located close to the heterochromatin of the proximal X chromosome, adjacent to other mapped mutations in the region. *wap* appears to be allelic to *CG14614* based upon the precise recapitulation of the viability and TDT *wap* phenotypes when *CG14614* was knocked down. The knock down of *CG14614* did not recapitulate the wing vein phenotypes that was observed in a subset of *wap* mutants, but since the wing vein phenotype is not fully penetrant, it is most likely that we have simply yet to sample sufficient flies to observe this effect. In addition, many of the flies that do eclose fail to expand their wings, making it difficult to determine if the subtle wing vein defect is present.

Having identified the gene responsible for the *wap* mutation, I next sought to determine the basis of the TDT phenotype.

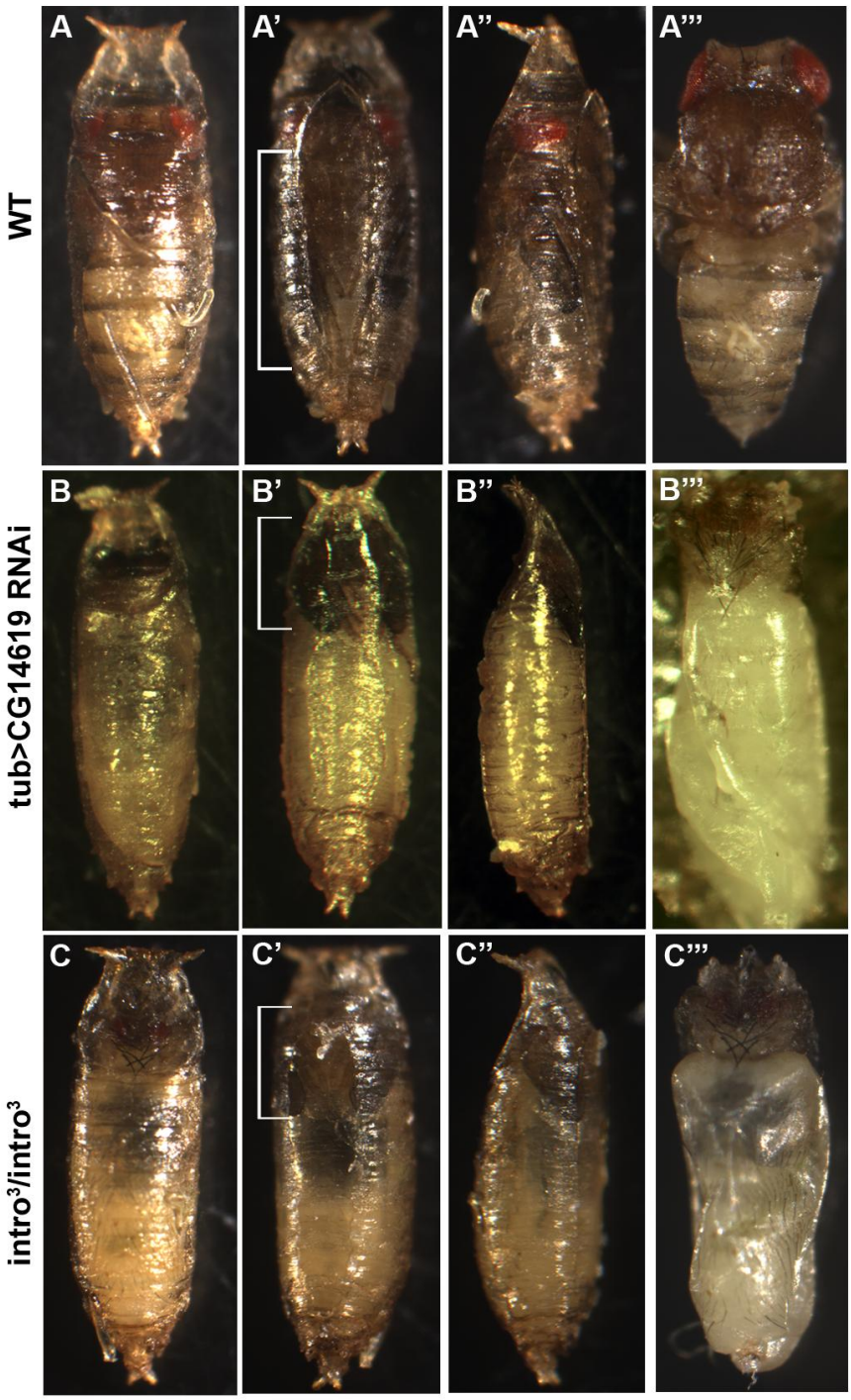

Figure 7: Knock down of *CG14619* recapitulates the phenotype observed in intro mutants. (A-A'') Dorsal, ventral, and lateral view of wild-type flies in the pupal cases shows normal development of the head, wings, and legs in the pupal case. (A''') When the pupa is removed from the pupal case, the fly resembles a fully formed adult. (B-B''') Knockdown of *CG14619* results in failure of head eversion and wing and leg extension. The pupa has only two observable body segments, the abdomen and thorax. (C-C''') *intro* homozygous mutants exhibit the same phenotypes as those seen in *CG14619* knockdowns.

TDT founder cells are specified early in development in *wap* mutants but are later lost

Muscle founder cells are required for proper specification of individual muscles. Since these cells have all the genetic information to give the muscle its unique identity, and since the *wap* mutant phenotype is specific to the TDT, we hypothesized that TDT-specific founder cells are not specified in *wap* mutants. The wap^{2} and wap^{9} mutations were recombined with the founder cell *duf-lacZ* line (also referred to as rP298) that shows *lacZ* expression in all muscle founder cells. Next pupae were dissected at 4 hour intervals beginning at 16 After Puparium Formation (APF) and flanking the early stages of TDT development (Fernandes and VijayRaghavan, 1993). Dissected samples were stained for the myoblast nuclei marker MEF2 (red) and β-Gal expressed by the rP298-*lacZ* marker of founder cell nuclei (green). Our results indicated that founder cells were specified early in development but were later lost (Figure 8).

In 16 hr APF *FM7i/rP298-lacZ,wap* heterozygous females, although the founder cells cannot be seen, the TDT is found located between DVM I and DVM II that were used landmarks for the presumptive location of the TDT (Figure 8A). In *rP298-lacZ,wap/Y* mutant males, the developing TDT muscle was present next to the DVM I (Figure 8B). At 20 hr APF, the TDT in *FM7i/rP298-lacZ,wap* pupae have more structured musculature and the presence of founder cells were evident in the TDT (green labeled cells, Figure 8C). By contrast, the 20 hr APF *rP298-lacZ,wap/Y* males had largely reduced staining of TDT-specific founder cells but did not exhibit a reduction in founder cell staining in the DVMs (Figure

8D). In addition to this, the mutant TDT (Figure 8D) is much less structured compared with the ordered nature of the wild-type TDT (Figure 8C). By 24 hr APF, the *FM7i/rP298-lacZ,wap* pupal musculature had a well developed pattern with the TDT nestled between the DVMs (Figure 8E). By contrast, in the 24 hr APF mutant *rP298-lacZ,wap/Y* males, the TDT is completely absent (Figure 8F).

The results of this study demonstrate the requirement for *wap* early in TDT development. Although specification and myoblast fusion are initiated in *wap* mutants, development cannot be sustained and TDT degeneration occurs. I next examined the cause for the degeneration of the TDT at so early a stage of development.

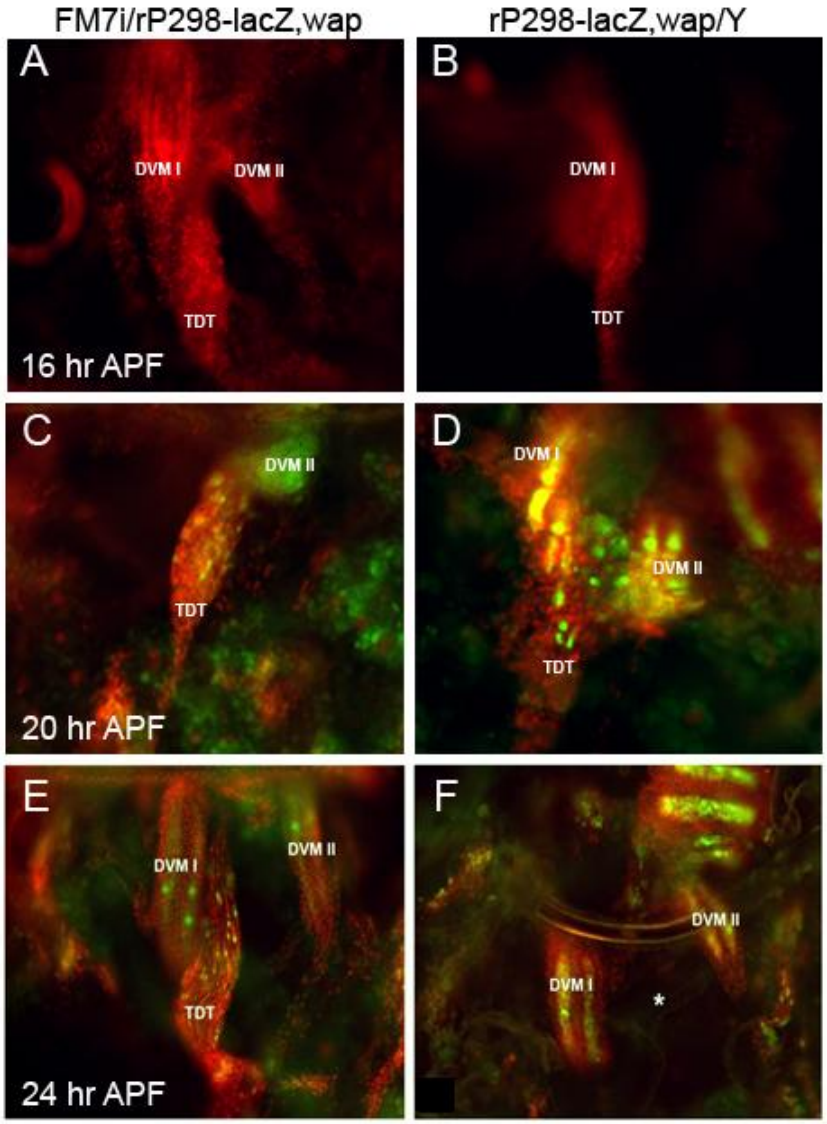

Figure 8: Founder cells are specified early in development but are later lost in wap mutants. (A, B) Formation of the TDT at 16 hours APF indicates that development of the TDT in wild-type (A) and *wap* mutants (B) is normal at this stage. (C, D) At 20 hours APF, the developing TDT in wild-type flies (C) is more structured than the TDT of *wap* mutants (D). The number of TDT-specific founder cells in the mutant is reduced compared to wild-type, even though there is no reduction in the founder cells of adjacent muscles. (E, F) By 24 hour APF, the mature TDT in wild-type flies (E) is well developed. By contrast, the TDT of *wap* mutants is absent (asterisk in F).

The Posterior Dorsal Mesothoracic Nerve (PDMN) reaches its intended muscle target, the TDT

My results indicated that the TDT is initially formed early in development but degenerates due to loss of TDT-specific founder cells. Adult muscle formation and neuron restructuring proceed in parallel with one another and the two processes are also dependent on one another. In studies of IFM development, when neuron restructuring is disrupted, the intended muscle target degenerates (Fernandes and VijayRaghavan, 1993). For this reason, we assessed whether the Posterior Dorsal Mesothoracic Nerve (PDMN), which innervates the TDT, is restructured properly. Since the innervation pattern is first observed at 18 hours APF and does not change markedly afterwards (Fernandes and VijayRaghavan, 1993), the correspondence of this process with the time points at which *wap* mutant phenotypes were apparent further supported neuronal defects as a possible mechanism for the *wap* TDT phenotype. Therefore, I dissected pupae at this stage from *wap/Y* males and compared the innervation pattern (visualized with anti-22C10, marking *Futsch* expression) with heterozygous *FM7i/wap* females. Figure 9 shows a normal innervation pattern for the TDT indicated by the arrow in the heterozygous *FM7i/wap* females. The PDMN reached the TDT in *wap/Y* mutant male pupae; however, the morphology of the nerve endings in the mutants differed from those of the heterozygotes. The nerves appeared to spread over the muscles but the boutons at the neuromuscular junctions appear to lack the structure observed in the wild-type neurons.

To visualize if these neuromuscular junctions (NMJs) are indeed absent in *wap* mutants, pupae were again dissected but visualized with anti-HRP (green) to observe the neurons, and anti-Dlg (red) to stain the muscles and NMJs (Figure 10). In the heterozygous *FM7i/wap* females, the nerves were visible and the HRP and Dlg antibodies were co-localized along the muscle. In contrast, the neurons of the *wap/Y* mutants were visible but did not make contact with muscles as indicated by the lack of co-localization of the HRP and Dlg. These results suggest that the NMJs are not properly formed in *wap* mutants. Since proper muscle formation is dependent on interactions between the developing muscles and nerves, the failure to form neuromuscular junctions may be the mechanism by which the *wap* mutation affects TDT development.

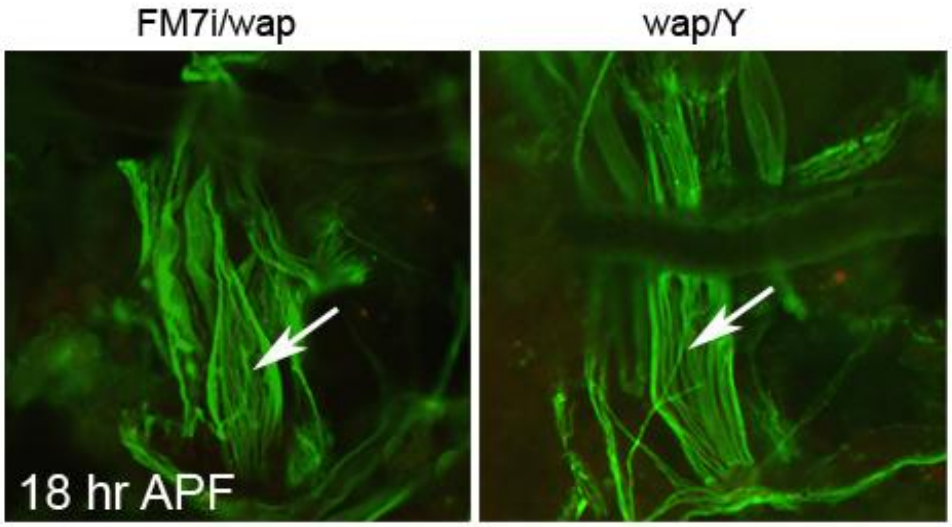

Figure 9: The Posterior Dorsal Mesothoracic Nerve (PDMN) is restructured to reach the TDT. 18 hour APF pupae were dissected and stained with anti-22C10 to label neurons and adult muscle. The stereotypical branching pattern of the PDMN is indicated by the arrow in the wild-type pupa. In wap mutant, the PDMN reaches the TDT but the morphology of the nerve branches does not reflect the characteristic pattern of the PDMN.

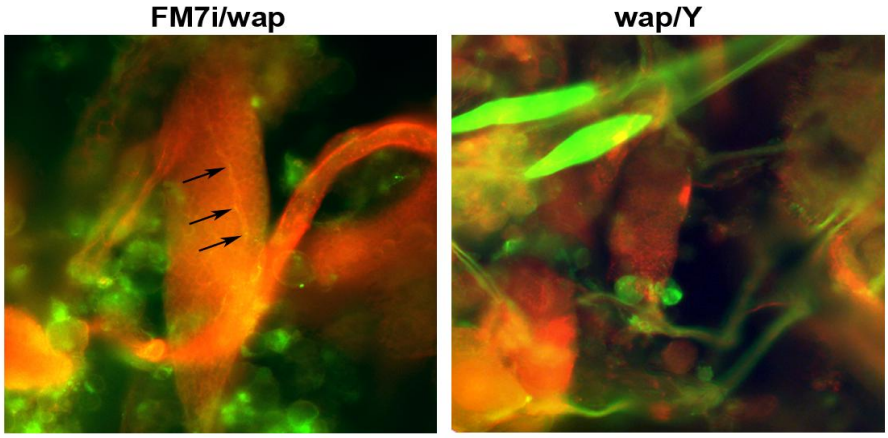

Figure 10: Neuromuscular junctions (NMJs) are not observed in *wap* mutants. In wild-type, the presence of NMJs are visible by the co-localization of HRP (green) and Dlg (red) indicated by the arrows. There is no co-localization of HRP and Dlg in *wap* mutants, indicating the NMJs are not properly formed.

Discussion

Different genes that exhibit similar mutant phenotypes often function within the same signal transduction pathway. Such signaling pathways require robustness to resist changes both in the environment and in the cells where the signaling is taking place. Without such robustness, development does not proceed normally. Mutants with observable phenotypes typically exhibit a complete breakdown of the signaling pathways that control proper development of the affected tissue types (reviewed in Friedman and Perrimon, 2007). Two distinct cell types, wing crossveins and adult muscles, each require the function of the same signal transduction networks for proper development (Jaramillo *et al*., 2009, Khalsa *et al*., 1998, Ralston and Blair, 2005). Known mutants with wing crossvein defects were therefore screened to identify potential defects in the morphology of the *Drosophila* jump muscle.

The *wings apart* mutant analyzed in this study exhibits an observable phenotype that affects not only the adult wing, but also the viability of the flies

and the formation of the TDT muscle. The observed TDT phenotype is similar to that of *crossveinless* (*cv*, FBgn0000394) mutants and other TGF-β mutants (Jaramillo *et al*., 2009) but does not exhibit the same wing crossvein phenotype as in those mutants. Since *cv* mutants that lacked the posterior crossvein of the adult wing also showed decreased numbers of TDT muscle fibers, and *wap* mutants have extra wing crossveins, we initially expected the *wap* mutants to have increased fiber number in the TDT. However, the observed downregulation of TDT formation by the *wap* mutant can be explained by at least two different possibilities.

The first possibility is that *wap* is involved in the TGF-β signaling pathway, like *cv*, but may interact with components of the pathway that do not interact with *cv*. The TGF-β pathway has many different ligands, different types of receptors, and various intracellular components that associate with each other in varying combinations in a context dependent manner (Khalsa *et al*. 1998). *MAN1* (FBgn0034964) protein products antagonize the TGF-β pathway (Wagner *et al.*, 2010) and *MAN1* mutation leads to the presence of ectopic wing crossveins (Pinto *et al*., 2008). These mutants do not have an observable muscle defect or abnormal neuromuscular junctions but affect synaptic transmission, providing further evidence for context dependence in TGF-β signaling activity.

A second possibility is that, although *wap* acts on the same tissues as *cv* and other TGF-β components, it may be part of a different signaling pathway. The *Epidermal Growth Factor receptor (Egfr*, FBgn0003731) pathway is also required for the proper formation of wing crossveins (Ralston and Blair, 2005)

and also functions in the formation of muscles (Maqbool and Jagla, 2007). Angulo *et al*. (Angulo *et al*., 2004) show that *absent, small, or homeotic discs 2* (*ash2*, FBgn0000139) represses EGFR signaling. Mutations in *ash2* also result in ectopic wing veins (Angulo *et al*., 2004) and neural defects (Beltran *et al*. 2003).

Other options are that *wap* functions in multiple pathways or act with sets of genes that are activated multiple times throughout development (Friedman and Perrimon, 2007). The only way to distinguish among these possibilities is to identify the transcriptional unit that is mutated to produce the observed phenotypes. In our initial mapping experiments, two deficiency lines were utilized that were induced using the FLP recombinase as described in Parks *et al*. (Parks *et al*. 2004) and thus has molecularly mapped breakpoints. The breakpoints for the other deficiencies were determined by cytogenetic analysis of X-ray induced deficiencies (Schalet and Finnerty, 1968, Schalet and Lefevre, 1973, and Rahman and Lindsley, 1981) and computed breakpoints were obtained from FlyBase (FB2012_02). Due to the presence of intercalating β-heterochromatin found within the proximal region of the X chromosome and the error commonly associated with imprecise breakpoint estimates in cytogenetic mapping (reviewed in Schalet and Lefevre, 1973, and Matthew *et al.*, 2009), assumptions made based on deletions with cytogenetically determined breakpoints may not be entirely accurate.

In this study, evidence for such inaccuracy was obtained. For example, initial mapping based solely on these deficiency chromosomes suggested that *DIP1* was the candidate gene model mutated in *wap* flies. However, additional

complementation mapping, using deficiency chromosomes, point mutations and duplications, and other published results (Kavlie *et al*. 2010), *DIP1* was excluded as the transcriptional unit for the *wap* gene. I was unable to definitively map the breakpoints of the deficiencies and the other mutations used in this study but closer estimates of the breakpoint and mutation locations were obtained by the combined conclusions of the cross results. In order to molecularly define the breakpoints, deep sequencing, using NextGen sequencing techniques, of the X chromosome in the deficiency lines is necessary. However, the refined mapping results suggest *wap* is located within the region between the *tilB* and *l(1)G0196* genes (genomic coordinates X:21,851,573…X:21,889,016.

Using RNAi analysis and the pupal semi-lethality phenotype of *wap*, I was able to rule out two of the six genes found in this region, *CG14618* and *CG12576*. In addition, by characterization of the thoracic muscles in the region, we were able to determine that the gene responsible for the *wap* phenotype was *CG14614*. *CG14614* is lethal in the late pupal stage during which *wap* mutant lethality is observed (Schalet, 1972), as well as the period in which wing crossveins develop (Waddington, 1940).

Temporal expression profiles for *CG14614* indicate moderately high to high expression in the embryonic stages beginning at 0 hours and decreasing through 16-18 hours (Graveley *et al*., 2011). Expression returns to moderately high levels in the late L3 larval stage and maintains this level of expression through day 3 of the pupal stage (Graveley *et al*., 2011). Formation of larval and adult somatic musculature, respectively, and peak expression of clusters of

muscle differentiation genes are expressed during these times (Arbeitman *et al*., 2002).

CG14614 is a gene that encodes a WD40 repeat domain protein with orthologs found in organisms ranging from yeast to plants, such as the TTG1 gene that regulates root, shoot, and leaf patterning in *Arabidopsis* (Walker *et al*., 1999, FlyBase, FB2012_02), to vertebrate craniofacial and muscle patterning genes (Nissen *et al*., 2006, FlyBase, FB2012_02). WD40 repeat proteins mediate protein-protein interactions and contain 4-10 repeating units of 44-60 residues ending in tryptophan and aspartate (WD) (reviewed in Holm *et al.*, 2001 and reviewed in Suganuma *et al*., 2008). These repeats form propeller-like structures, termed β-propellers, created by the folding of four antiparallel β-sheets (reviewed in Holm *et al*., 2001). This protein family is known to have roles in signal transduction, mRNA processing, gene regulation, vesicular trafficking, and regulation of cell cycle (reviewed in Skurat and Dietrich, 2004 and reviewed in Suganuma *et al.*, 2008).

One particular vertebrate ortholog for *CG14614*, is the vertebrate *wdr68* gene that is involved in craniofacial patterning in zebrafish (Nissen *et al.*, 2006) but has also been isolated in rabbit skeletal muscle (Skurat and Dietrich, 2004). The zebrafish severe craniofacial defect observed in *wdr68* mutants can be rescued by *CG14614* suggesting that the function of the *wdr68* gene is conserved in animals from invertebrates to vertebrates, even in developmental processes not found in the invertebrate animals (Nissen *et al*., 2006).

Wdr68 associates with members of the Dual-specificity tyrosine phosphorylation-regulated kinase gene family, Dyrk1a and Dyrk1b. Dyrk1a plays a role in phosphorylation of glycogen synthase and is expressed at high levels in the central nervous system, heart and skeletal muscle (Skurat and Dietrich, 2004). Mutations in *Dyrk1a* genes in humans and mice are associated with neurological defects (Martinez de Lagran *et al*., 2004). *Dyrk1b*, which is activated by Rho-GTPase family members, has increased expression in skeletal muscles and regulates the transition from growth to differentiation. Knockdown in mouse C2C12 cell lines displays a loss of myogenin expression and leads to failure in muscle differentiation (Deng *et al*., 2003). Dyrk1 also has a conserved function between vertebrates and invertebrates. The *Drosophila* gene *minibrain* (*mbn*) is a functional ortholog of the vertebrate *Dyrk1a* and is shown to be required in proper formation of post-embryonic neurons (Tejedor *et al.*, 1995 and reviewed in Kinstrie *et al*., 2006).

The Wdr68/Dyrk1 complex is required for proper differentiation of multiple tissues in a conserved manner and cellular localization of this complex is dynamic (reviewed in Nissen *et al*., 2006). Moreover, given that the WD40 repeats contained in the Wdr68 protein can facilitate protein-protein interactions (reviewed in Holm *et al*., 2001), it is possible that the Wdr68/Dyrk1 complex functions as part of a signaling pathway. It is unknown whether *mbn* is localized in the same tissues as *wap* (*CG14614*) and whether the two proteins genetically interact in *Drosophila* as do their vertebrate homologs. Further analyses such as *in situ* hybridization and immunostaining of flies for *wap* and *mbn* are necessary

to resolve whether the gene products are colocalized in the developing adult muscle or neurons in *Drosophila* pupae. In addition, much work is needed to characterize *CG14614* in the context of the *wap* mutation.

Based on our data, CG14614 is the gene that gives rise to the *wap* phenotype. In order to confirm these results, rescue of *wap* by the protein encoded by *CG14614* will be performed. The initial rescue of the *wap* mutation was performed using a large duplication of the X chromosome. Since gene expression of the *CG14613* gene was not tested by RNAi, this is a necessary step to ensure *CG14613* is not also involved in the phenotype of the *wap* mutation. It would also be interesting to determine if the *wap* mutation can be rescued by zebrafish Wdr68 protein in a reciprocal rescue experiment to that performed by Nissen *et al*. (Nissen *et al*., 2006). It is also important to determine where the *wap* mutations are located in the *CG14614* gene. Sequencing of the *CG14614* gene in the *wap* mutants is necessary for further analysis of this mutation, to define its role in muscle development, and to understand its molecular mode of action.

The RNAi results not only allowed the ubiquitin-specific protease encoding gene *CG14619* to be ruled out as the gene affected by the *wap* mutation but also helped identify this gene as the most likely gene responsible for the *intro* mutation. At the end of the larval stage, a pulse of ecdysone is released, inducing pupariation and the onset of metamorphosis (Thummel, 1996). At 12 hours APF, another pulse of ecdysone is released, resulting in contractions of the abdomen allowing the prepupa to move posteriorly to make room for the head in the

anterior end of the pupal case. This contraction creates internal pressure that causes head eversion and final elongation of the wings and legs (reviewed in Forier *et al.*, 2003). The pupae from the RNAi knock downs displayed failure of head eversion. The presence of the head structures can be seen in the thorax sections in Figure 6. In the phenotype observed in Figure 7 the *tub-Gal4/CG14619* (37929), the pupa is characterized by only two visible body segments, the abdomen and thorax. The results of *tub-Gal4/CG14619* (37930) RNAi knock down (not shown) were similar to those obtained for line 37929. The same phenotype can be observed in *intro* mutants.

This phenotype is reminiscent of the phenotype observed in ecdysone-response genes, such as β-FTZ-F1 (FBgn0001078, Fortier *et al*., 2003), and *cryptocephal* (*crc*, FBgn0000370) *(Hewes et al*., 2000). In these mutations, head eversion fails and, in some cases, there is a leg disc elongation defect (Hewes *et al*., 2000) that is also observed in *CG14619* knockdowns. Before the conclusion can be made definitively that *CG14619* is the most likely gene affected by *intro* mutants, rescue of the *intro* phenotype by expression of *CG14619* protein is necessary. The lines used in this study both had off-target hits to 23 genes other than *CG14619*, some of which can also be induced by ecdysone. Whether the phenotype we are seeing is the result of knockdown of *intro* or the result of knockdown of another target is still unknown. While it is possible that the phenotype observed may be due to off-target hits by the RNAi constructs used, the recapitulation of the phenotype observed in the *intro* homozygous mutants suggest this is unlikely. Another way to address this problem is to knock down

expression of *CG14619* with a different RNAi construct with no off-targets to determine if the same phenotype is observed. Nevertheless, the potential function of *CG14619* in head eversion identifies it as a possible genetic target of one of the *cryptocephal* genes, each of which encodes regulatory proteins.

To determine a mechanism by which *wap* affects the development of the TDT, I first analyzed whether TDT-specific founder cells are specified in these mutants. Founder cells provide the unique identity of individual muscles Specification of muscle founders is dependent on intrinsic expression of genes and extrinsic signaling pathways acting on the cells in combinations that are unique for each specific muscle (reviewed in Maqbool and Jagla, 2007). These cells can competently form thin muscles at properly specified locations even when fusion of additional myoblasts fails to occur (Dutta *et al*., 2004) further suggesting that these cells are important components of proper muscle development. When we observed the development of the TDT over time, we found that the muscles begin to form normally and include the presence of TDT-specific founder cells, marked by expression of the rP298-*lacZ* transgene. As development progresses, we observed a loss of founder cells and a subsequent disorganization of the TDT by 20 hrs APF, followed by degeneration of the TDT by 24 hrs APF.

Muscle identity is not only determined by founder cell specification, it is also determined by its innervation pattern. The innervation of a specific muscle is stereotypical and therefore exhibits a precise and unvarying wiring pattern (Keshishian, *et al*., 1996). As development progresses, the growth cones of the

motor neuron explore the surfaces of myotubes, searching for the correct synapse partner. To accomplish specific targeting of the motor neuron, cell surface molecules must be expressed on the founder cells (reviewed in Keshishian *et al*., 1996). In the absence of founder cells, defasciculation of axons is inhibited and neurons do not branch to reach their targets (Landgraf *et al*. 1999). The final step of innervation of a muscle target is the formation of the synapse (reviewed by Shishido *et al*., 1998). Synapse formation requires proper formation of both the pre-synaptic active zones and differentiation of the post-synaptic muscle (Prokop *et al*., 1996). Studies involving the dorsoventral muscles of the adult thorax indicated that ablation of the nerve that innervates these muscles blocks formation of muscle fibers, even though myoblast fusion was initiated. These results suggest that interaction between the nerve and its postsynaptic muscle target are critical for maintenance of the synapse and therefore for proper formation of the muscle (Fernandes and Keshishian, 1998).

Results from this study show that formation of the PDMN occurs normally and reaches its target. Morphology of the neuron branches in *wap* mutants is not the same as that observed in the wild-type. Based on this morphology, we determined if the NMJs are properly formed in the mutants. In wild-type pupae, NMJ formation was observed, however, synapses were not apparent in the *wap* mutants. These results suggest the mechanism by which *wap* affects development of the TDT is failure of proper motor neuron synapse formation. It is still necessary to determine whether this effect is due to a defect in the presynaptic neuron or the postsynaptic muscle. To determine this, tissue specific

knockdown of the identified *wap* gene, *CG14614* will be performed in the muscle, using the myoblast *1151*-Gal4 driver, and also in the neuron, using the *elav*-Gal4 driver.

This tissue-specific analysis is crucial to understanding what effect this gene has on the development of the muscles. Since orthologs of *CG14614* and their interaction partners are found in both skeletal muscle and nerves (Skurat and Dietrich, 2004), the effect could potentially be on either side of the synapse.

The relevance of understanding the effects of the *wap* mutation may not be immediately apparent in terms of the specificity of the *Drosophila* muscle it affects. However, this study indicates *CG14614* has an evolutionarily conserved function, which is consistent with the findings that the *Drosophila* gene can rescue genetic defects found in vertebrates (Nissen *et al*., 2006). Thus, this system may allow us to determine how *CG14614* and its vertebrate homologues function in establishing formation of muscle and neuromuscular junctions. Insights gleaned from vertebrate models have indicated that muscle degeneration/atrophy results from improper formation of neuromuscular junctions, even when neurons reach their intended targets (Williams *et al*., 2009). Furthermore, neuromuscular junctions are conserved from flies to humans at the genetic, molecular, and physiological levels (Lloyd and Taylor, 2010). Nervous system involvement is frequently found in different muscular dystrophies (reviewed in Guyon *et al*., 2007) making it important to study the molecular basis of these diseases in organisms that can facilitate a basic understanding on the processes involved.

CHAPTER 2

TRANSCRIPTIONAL REGULATION OF THE EARLY MESODERMAL *MEF2* ENHANCER BY TWIST AND MAD

Abstract

Mesoderm formation is one of the key events in early development of organisms from invertebrates to vertebrates, and the resulting germ layer gives rise to diverse cell fates. *Myocyte Enhancer Factor 2* (*Mef2*) is required for proper formation of the mesoderm and all lineages of muscle. Expression of *Mef2* must be tightly regulated to ensure precise spatiotemporal activity of the gene throughout the developmental process. A 1,059 base pair enhancer is required for proper expression of *Mef2* in the developing dorsal mesoderm that eventually forms the visceral muscle, dorsal somatic muscles, and heart. In this study, we assess the contributions of the transcription factors Twist and Mad/Medea to *Mef2* expression via this enhancer. Activation of the enhancer requires both Twist and Mad/Medea binding sites *in vivo*. Moreover, these transcription factors can activate the enhancer in tissue culture, although not synergistically. The transcription factor Dorsal may also interact with this enhancer to facilitate both activation and repression of *Mef2* activity. These studies define the enhancer that regulates expression of *Mef2* in the developing mesoderm and the contributions of Twist and Mad to enhancer activation. The study also highlights the complexities of mesodermal *Mef2* enhancer activation *in vivo*.

Introduction

Coordinated inputs of signaling and transcription networks allow for acquisition of specific cell fates during embryogenesis (Sandmann *et al.*, 2007). Proper development of the mesoderm is critical for the developing embryos of all triploblastic animals. The mesoderm is the middle germ layer of the developing

embryo composed of pluripotent cells that give rise to the somatic, visceral, and cardiac muscles. Its development is initiated by high nuclear concentrations of the transcription factor Dorsal in ventral cells of the embryo which, in turn, activates the *twist* and *snail* genes. Activation of twist and snail lead to the induction of gene expression critical for the maintenance and further development of mesodermal tissues (Leptin *et al*., 1991).

Mef2 is activated early in the developing mesoderm and is required for proper development (Sandmann *et al.*2007). MEF2 is part of the Myocyte Enhancer Factor 2 family of transcription factors containing a MADS (MCM1, Agamous, Deficiens, serum response factor) domain that binds to the regulatory region of myogenic and muscle structural genes (reviewed in Cripps and Olsen 2002). M*ef2* is the only gene known to regulate the entire muscle differentiation process, including both the spatial and temporal distribution of myogenic cells, and is expressed in precursors to all muscle lineages. Early in development, it is expressed throughout the mesoderm.

After gastrulation, MEF2 is also found ubiquitously within the mesoderm and after the mesoderm layer spreads to the dorsal region, *Mef2* is enriched at the dorsal region of the embryo. This suggests that there is very stringent regulation of *Mef2* in both the early and late stages of development (Nguyen and Xu 1998). There are at least twelve different upstream enhancers of *Mef2* that direct the differential regulation of this gene in the various tissues and developmental stages (reviewed in Black and Olson, 1998). One such *Mef2* enhancer active early in mesoderm development is regulated by the transcription

factor Twist (Cripps *et al.* 1998) and later by the Mad and Medea transcription factors (Nguyen and Xu 1998). This early mesodermal enhancer is approximately 4 Kb in length (from position -3564 to +521). A core portion of this sequence is active in imaginal discs, controlled by a 175 bp region, and regulates adult somatic muscle precursors. However, the minimal 175-bp enhancer is not fully active in the embryonic mesoderm (Cripps *et al.* 1998).

Twist is a basic helix-loop-helix (bHLH) transcription factor that specifically binds to E-box consensus sequences (CANNTG) and directly activates *Mef2* (reviewed in Castanon *et al*., 2001). The 175 bp early *Mef2* enhancer contains two E-box sites in *Drosophila melanogaster*, each of which has conserved locations between *D. melanogaster* and *D. virilis*. Of these E-box sites, E1 is identical in sequence between the two organisms and E2 has a differing core sequence. In adult muscle precursors, E1 is essential for *Mef2* expression (Cripps *et al.* 1998). A loss in Twist binding to this site and not the others results in loss of enhancer activity. It is, however, unknown whether *Mef2* is directly activated by Twist at the early mesodermal stage because even when E1 is mutated, there is still weak, non-uniform expression of *Mef2* in the developing mesoderm and the enhancer is not fully active when Twist is uniformly present. At this stage of development there may be other enhancer sequences outside the 175 bp *Mef2* enhancer that are active in adult muscle precursors (Cripps *et al.* 1998). It is possible that Twist acts in combination with other factors to regulate *Mef2* throughout early mesodermal development, but this has not yet been established. As it has been shown by Nguyen and Xu (1998), the

mesodermal *Mef2* enhancer contains binding sites for Mad/Medea transcription factors. However, it has not been determined if these sites are important for proper enhancer activity.

Mothers against dpp (Mad) and Medea (Med) are members of the Smad family of transcription factors that transduce signals from receptors of the TGF-β family proteins to promoters of target genes. Mad is an ortholog of mammalian Smad 1/5 and Med is an ortholog of mammalian Smad4 (Massague *et al.* 2005, Wisotzkey *et al.*1998). Smad1/5 is an example of a receptor-regulated Smad (R-Smad) that interacts with Smad4, Co-Smad, upon activation by a TGF-β receptor. This complex migrates into the nucleus and binds DNA at Smad-binding elements (SBEs) containing the core GTCT sequence via a β-hairpin structure in one domain of the protein (Massague *et al*. 2005). The binding affinity at a single SBE is too low for Smad complex binding and it has been found that many Smad-binding promoter sequences have multiple SBEs (Shi *et al.* 1998). Having multiple SBEs is likely to allow for tighter binding of the Smad transcriptional complex and also may require additional factors in the complex to effectively bind DNA (Seoane *et al*. 2004). Some Smads can also interact with the GC rich sequence GCCGnCGC (Xu *et al*. 1998). The mesodermal *Mef2* enhancer region has three GC-rich regions that are capable of binding Mad and Med. It has not yet been established whether the three Mad/Med sites are functionally important or whether there are mesodermally expressed transcription factors, such as Twist, which can act synergistically with the Mad/Med complex to induce Mef2 expression (Nguyen and Xu 1998).

This study aims to determine how the transcription factors Twist, and Mad/Med interact in the enhancer region of the *Mef2* gene to regulate early development of the mesoderm. In order to accomplish this goal, the binding capabilities of Twist are initially verified using electrophoretic mobility shift assays (EMSAs), whereas previously performed analyses for the Mad/Med sites have already confirmed that Mad/Med binds to all three sites of the *Mef2* enhancer (Nguyen and Xu 1998). *In vivo* studies using P-element mediated germ-line transformation are then conducted to determine the functional significance of each of the binding sites on the *Mef2* enhancer region for the developing mesoderm. We also assess whether interaction between the transcription factors is required for the activation of the *Mef2* gene.

Materials and Methods

Generation and analysis of enhancer constructs

Transgenic DNA constructs for the *Mef2* early enhancer were generated using standard PCR methods. Primers were designed to amplify the *Mef2* enhancer region. The forward primer for all enhancer constructs was 5'-GGGAATTCAAGCTTGTTGGCTTGTCTTGGC. For the DM1, Twi1, and Mad3 constructs, the reverse primer was 5'-GATATTATTTACCTTAAACACGC. The reverse primer for the DM2 construct was 5'-GTTCTAACCCATATAGGAAATGATTTTGC. We used the reverse primer 5'-ATGATTTTGCGCCTATTTATAC for the generation of the DM3 fragment. Mutation in the first Twist binding site of the *Mef2* enhancer was induced using PCR-based site directed mutagenesis described by Horton *et al.* (Horton *et al*.,

1993) changing the Twist binding site from 5'-CACATGTG to 5'CGGCCGTG. Mutation of the three Mad/Med binding sites was performed by site-directed mutagenesis using the GeneTailor mutagenesis kit (Invitrogen), following manufacturer's instructions. The Mad1 binding site (GC-3 in Nguyen and Xu, 1998), was changed from 5'-CTGTGCGCCGTACGGTTGATGCTG to 5'-ATGAGCACCA, the Mad2 binding site (GC-2) was changed from 5'-GCCGCCCGGC to 5'-ACCACCAGGA, and the Mad3 binding site (GC-1) was changed from 5'-CCCTCGCCTCTCGGCGGCG to 5'-ACCACGACTATCAGCAGCA.

PCR products were cloned into pCaSpeR-hsp43-AUG-β-gal (CHAB) P-element transformation vector containing a *lacZ* reporter gene downstream of a minimal hs43 heat-shock promoter (Thummel and Pirrotta, 1992). P-element mediated germ-line transformation was performed as described by Cripps *et al*., (Cripps *et al*., 1999). Cloned constructs were injected into *y w* embryos and transgenic lines were identified in the G1. Independent lines were maintained by backcrossing to *y w* and selecting for homozygotes in subsequent generations based on darker eye color. A minimum of three independent lines were analyzed for each enhancer tested. Flies were raised in Carpenter's medium at 25^{o}C.

Immunohistochemistry

Embryos were collected and stained as described by Patel (1994). Primary antibodies were mouse anti-β-galactosidase 1:1000 (Promega). The Vectastain Elite Kit (Vector Laboratories) and diaminobenzidine (DAB) stain were used for secondary detection according to manufacturer's instructions. Samples

were mounted for photography using an Olympus BX51 photomicroscope with DIC optics, after being cleared in glycerol. Images were collected digitally and figures made using Adobe Photoshop.

Electrophoretic Mobility Shift Assay

Twist protein was generated using T7 polymerase and the TnT Coupled Transcription/Translation system (Promega) and pAR-Twist (Cripps *et al*., 1998). Two oligos of the sequence 5'-GGATGCACTCAACACATGTGCAACATGCGG-3' and 5'-GGCCGCATGTTGCACATGTGTTGAGTGCAT-3' were annealed and the 5'-GG overhangs filled with Klenow enzyme (New England Biolabs) and (α-^{32}P)dCTP to generate radiolabeled E1 probe DNA. Probes were purified on an illustra Autoseq G-50 Dye Terminator Removal Kit spin column (GE Healthcare) and 50,000 cpm were used in each assay. E2 wild-type binding site oligonucleotides have the sequence 5'-GGCGGATATACACACATGGATCGTTTGC and 5'-GGGCAAACGATCCATGTGTGTATATCCG. Wild-type sequences for the E3 binding sites are 5'-GGATTTAAATGCCATATGGTAATGGCTA and 5'-GGTAGCCATTACCATATGGCATTTAAAT. For competition experiments, wild-type E1 and mutant E1 oligonucleotides were used in the reactions at 100x concentrations. E1 mutant oligonucleotides were generated in the same way using the sequences 5'-GGATGCACTCAACACGGCGGCAACATGCGG and 5'-GGCCGCATGTTGCGGCCGTGTTGAGTGCAC. Mutant E2 oligonucleotide sequences are 5'-GGCGGATATACACCCGGGGATCGTTTGC and 5'-GGGCAAACGATCCCCGGGTGTATATCCG and mutant E3 oligonucleotides are

5'-GGATTTAAATGCGACGTCGTAATGGCTA and 5'-GGTAGCCATTACGACGTCGCATTTAAAT. Electrophoretic mobility shift assays (EMSAs) were performed using standard methods (Sambrook *et al*., 1989). Binding reactions were incubated at room temperature and gels were run at a constant temperature of 4^{o}C. Dried gels were subjected to autoradiography.

Cell culture and transfection

For co-transfections assays, the expression plasmid pBRAcPA-Tkv was generously provided by Michael O'Connor (University of Minnesota, Twin Cities). We cloned Mad cDNA from the RE72705 DGRC Gold expression plasmid (Stapleton *et al*., 2002) into pAW using Gateway Cloning Technology (Invitrogen) according to manufacturer's instructions. The expression plasmid pPac-Twi was also used in cell culture assays. Reporter constructs used for the P-element mediated germ-line transformation were used in cell culture experiments. SL2 cells were maintained at 25^{o}C in Schneider's *Drosophila* medium supplemented with 10% heat-inactivated fetal bovine serum (FBS) (both from Invitrogen). Cells were transfected as described in Kelly Tanaka *et al*. (Kelly Tanaka *et al*., 2008). The ratio of transcription factor coding DNA to reporter DNA used was 1:9. DNA was transfected into the cells using Cellfectin transfection reagent (Invitrogen). Each treatment was transfected into two well per trial for three trials.

β-galactosidase assays

β-galactosidase assays were performed in transfected cells using a mammalian β-galactosidase assay kit (Pierce Biotechnology) according to manufacturer's recommendations as described in Kelly Tanaka *et al*. (Kelly

Tanaka *et al*., 2008). Sample absorbance was read at 405 nm in an OpsysMR multiplate reader (Dynex Technologies) warmed to 37^{o}C. Five absorbance measurements were taken at ten minute intervals beginning with t=0. Assay plate remained incubating in the plate reader between measurements. Activation folds were measured as the average of the measured β-galactosidase activity over time, normalized to non-transfected cells. Standard error was calculated for each activation fold and statistical comparisons between treatments were determined by Student's t-test.

Results

Earlier studies suggested that the *Mef2* enhancer that is capable of directing expression in the entire mesoderm is located from -3572 to +521 (Cripps *et al*., 1998). A study by Nguyen and Xu (1998) also indicated that the early mesoderm and dorsal mesoderm enhancers are located in smaller regions than reported full mesoderm expression of *Mef2*, of sizes 280 bp and 460 bp, respectively (Nguyen and Xu, 1998). Successive 5' and 3' deletions of the mesoderm enhancer were performed by Cripps *et al*. to determine what upstream regulatory region is necessary for expression of the *Mef2* dorsal mesoderm enhancer (Cripps *et al*., 1998). It was determined that a 1,059 base pair region within the *Mef2* enhancer described by Cripps *et al*. (1998) is necessary for expression of *Mef2* in the developing dorsal mesoderm (Figure 1A).

The 1,059-bp enhancer region was cloned into pCaSpeR-hs43-AUG-β-gal (CHAB) and its *lacZ* expression was tested in the developing embryo. *Mef2*

enhancer activity was present in the dorsal mesoderm (Figure 1B), and to some extent, the early mesoderm (not shown). Interestingly, in an 848 base pair enhancer fragment with 211 base pairs removed from the 3' end, all expression of the *lacZ* reporter was lost (Figure 1B). However, when another 20 base pairs were removed from the 3' end of the enhancer, some *Mef2* activity was restored in the dorsal mesoderm, but this activity was not quite as strong as that of the 1,059 bp enhancer (Figure 1B). These results suggest that the 1,059-bp enhancer is sufficient to drive expression of the *lacZ* reporter. Furthermore, the data suggest that the 211-bp at the 3' end of the enhancer is critical to enhancer activity and that there must be a repressor within the -1593 to -1573 region of the enhancer since enhancer activity is restored when this 20 bp region is deleted.

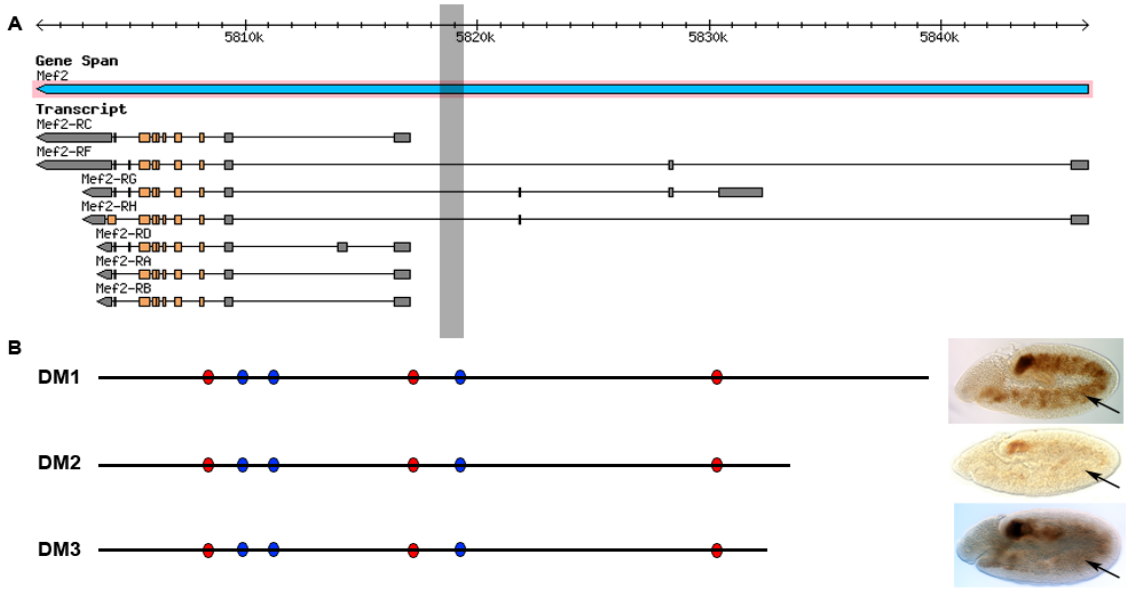

Figure 1: A 1,059 bp enhancer controls *Mef2* expression in the dorsal mesoderm. (A) Map of the *Mef2* gene showing the location of the mesodermal enhancer (gray highlighted region). (B) The 1,059 bp mesoderm enhancer DM1, regulates expression of *Mef2* in the dorsal mesoderm (arrow). Red circles on this map indicate the presence of E-box binding sites which bind the transcription factor Twist. Blue circles indicate the presence of three Mad/Medea binding sites located on the enhancer. Deletion of 211 bp from the DM1 enhancer creating an 848 bp enhancer, DM2, abolishes *Mef2* expression in the mesoderm. The DM3 enhancer contains an additional 20 bp deletion from this enhancer and restores some of the dorsal mesoderm expression of *Mef2*.

Three E box consensus sites were present in the 1,059 bp enhancer. Although only two of the E box sites are conserved I tested the ability of the bHLH transcription factor Twist to bind each of the sites. Twist lysate was generated by in vitro transcription and translation. As previously reported, Twist was able to bind specifically to the E1 binding site (Figure 2A). Unlabeled wild-type E1 probe was able compete for binding to the E1 site, but unlabeled mutant E1 probe was not, indicating that the interaction between Twist and the E1 site was sequence-specific. Twist was not able to bind the E2 site on the enhancer. The E3 site was not conserved in all species of *Drosophila* and was therefore not previously tested for ability to bind Twist. Our results show that Twist can bind this site, although not as strongly as it binds the E1 site (Figure 2A). This binding is specific since unlabeled wild-type probe can compete for Twist binding and mutant probe is unable to bind Twist. These results indicate Twist can bind two E box sites located on the mesodermal enhancer but that binding is stronger at the E1 site, suggesting this is the primary binding site occupied by Twist.

To determine the functionality of the Twist binding sites, I generated an enhancer fragment (Twi1) in which we mutated the E1 site of the 1,059 bp construct, since Twist exhibited the highest affinity for this site. This fragment was cloned into the CHAB vector and injected into embryos to assess *Mef2* expression in this mutant construct (Figure 2B). When we analyzed *lacZ* expression of this transgenic line, we observed that enhancer activity was completely abolished by the mutation (Figure 2B). This suggested that not only is

this binding site required for dorsal mesodermal expression of *Mef2*, but that the presence of another binding site to which the Twist protein is able to directly bind, is not sufficient to compensate for the loss of the E1 site. This E1 site is the functional Twist binding site on the *Mef2* enhancer.

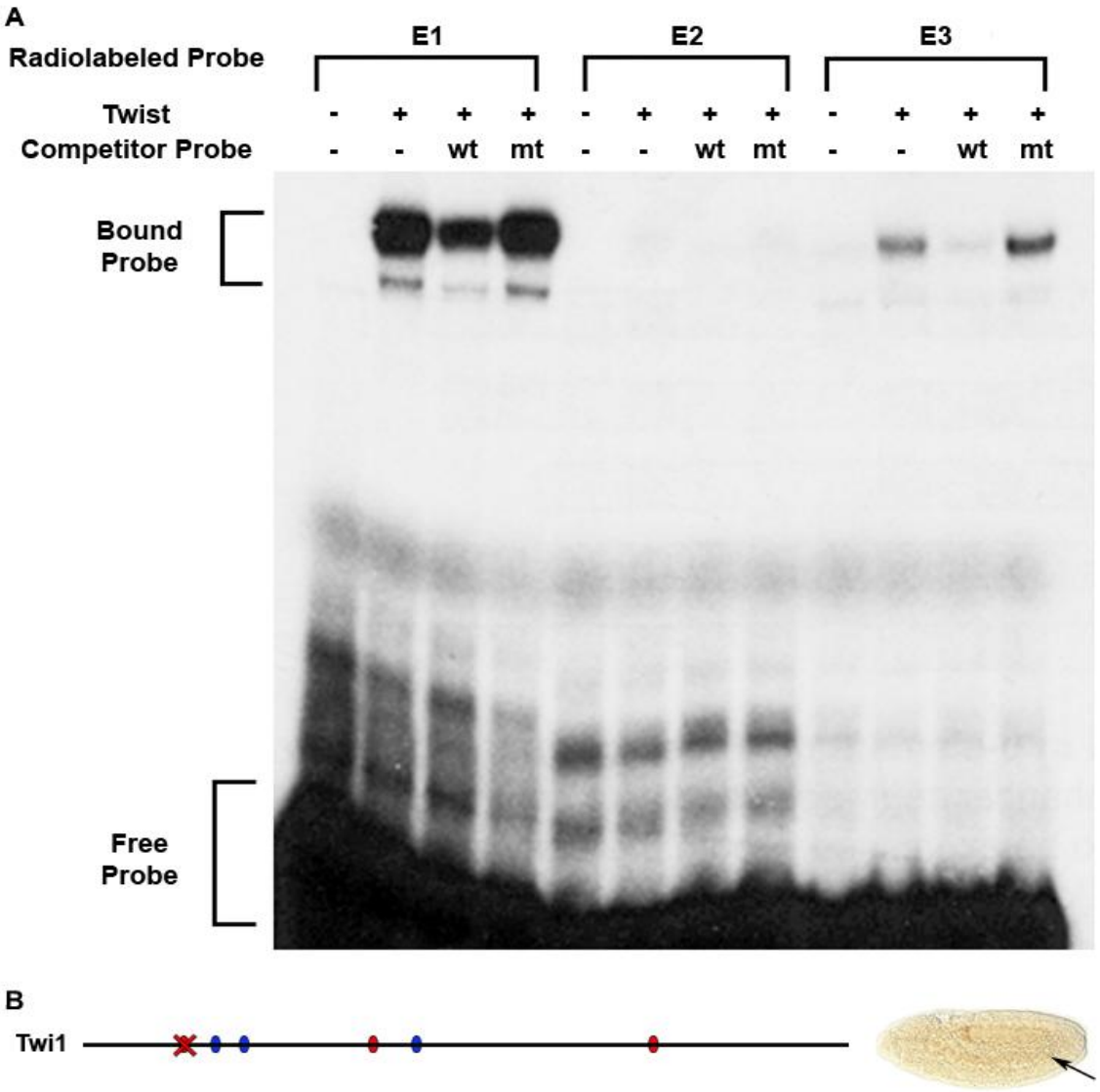

Figure 2: The E1 binding site is required for *Mef2* activity and directly binds Twist protein. (A) Electrophoretic mobility shift assay (EMSA) indicates direct, specific binding of Twist protein to the E1 and E3 binding sites of the *Mef2* enhancer. Binding to the E1 site is much stronger than binding to the E3 site. (B) Mutation of the E1 binding site on the *Mef2* enhancer ablates all mesodermal enhancer activity (arrow) and reveals a requirement for Twist binding to this site. The presence of the E2 and E3 binding sites cannot compensate for loss of binding to the E1 site.

Also found within this enhancer sequence are three Mad/Med binding sites. These sites can each specifically bind both Mad and Med protein, although the Med protein binds the Mad1 (denoted GC-3 in Nguyen and Xu, 1998) binding site with lower affinity than Mad. Additionally, this binding site does not exhibit the same specificity of binding Mad as do the other binding sites as it is not competed by unlabeled Mad1 (GC-3) probe as efficiently as this competitor probe competes with the other two sites (Nguyen and Xu, 1998).

Since Mad/Medea was able to bind all three binding sites to varying degrees and specificities, we generated a *Mef2-lacZ* line termed Mad3 with all three Mad/Med binding sites mutated to determine whether these sites are necessary for expression of the *Mef2* enhancer. These transgenic animals maintained some of the expression observed in the non-mutated 1,059 bp DM1 enhancer, but reporter gene expression was clearly reduced (Figure 3). These data are consistent with those reported by Nguyen and Xu in which the expression of *Mef2* is lost in mutants of the *dpp* signaling pathway (Nguyen and Xu, 1998), but more importantly it demonstrates that the Dpp signal is transduced through the identified sequences. It was suggested that residual expression of the *Mef2* enhancer in the *dpp* mutants could potentially be due to continued expression from earlier stages of development.

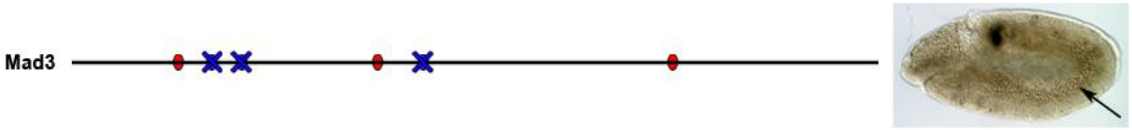

Figure 3: Deletion of Mad/Medea binding sites on the *Mef2* enhancer reduces dorsal mesoderm expression of *Mef2*. Although expression of *Mef2* is reduced when all three Mad/Medea sites are mutated, expression persists in the dorsal mesoderm (arrow).

Since Twist binds the enhancer directly and since Dpp signaling is necessary for *Mef2* enhancer activity, we examined the possibility of cooperative interaction of these factors in activating the mesoderm enhancer in a cell culture system. No activation for the 1,059 bp DM1 enhancer was observed for any of the transcription factors (Figure 4A). The activation folds in this experiment were less than 2, the threshold set by our method for activation. This is unexpected since the enhancer is able to activate expression in the embryo. In co-transfection experiments using the DM2 enhancer (Figure 4B), as expected, there was no activation of the DM2 enhancer as all levels for this enhancer were below the 1.5 fold activation level. When we tested the 828 bp DM3 construct, we saw similar activation levels with Twist and Mad alone as observed for activity levels in the DM1 construct (Figure 4C). The presence of Twist and Mad in combination did not result in much of a difference in the activation levels of the enhancer. Mad phosphorylation is required for translocation of Mad into the nucleus of the cell (reviewed in Wisotzkey *et al*. 1998). In order to ensure Mad was being translocated into the nucleus we co-transfected Mad with activated Thickveins receptor (Tkv, FBgn0003716). When we included this receptor in our cell culture experiments, activity of the DM3 enhancer was significantly increased from levels observed for Twist alone, Mad alone, and Twist and Mad in combination ($p<0.01$). There was no difference in the activation of Twist, Mad, and Tkv* in combination with each other from that observed when only Mad and Tkv* are present, suggesting these factors do not act together to drive

expression of the *Mef2* enhancer. Med did not influence activation of any line (data not shown).

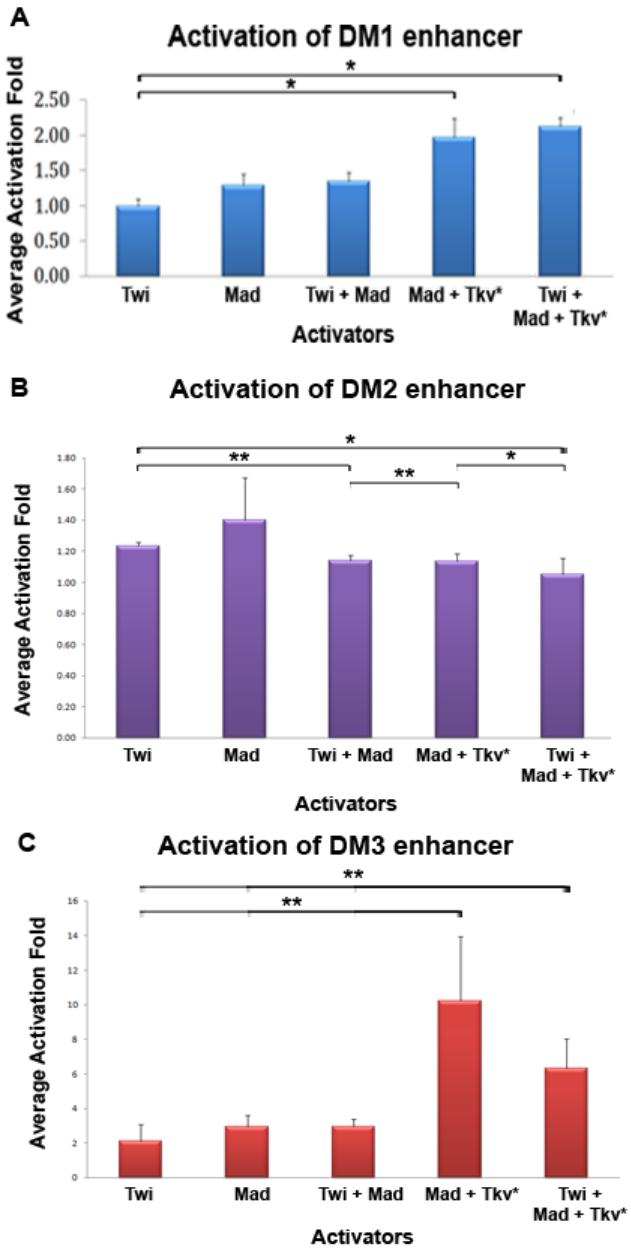

Figure 4: The DM3 enhancer is activated in *Drosophila* SL2 cells. (A, B) Activation fold levels for transcription factor treatments co-transfected with either the DM1 (n = 12) or DM2 (n = 6) reporter do not reach the threshold level to conclude these factors activate the enhancer. This suggests there is no significant difference in the ability of Twist or Mad alone or together to influence enhancer activity unless activated Thickveins (Tkv*) receptor is included in the co-transfections (A). All combinations of activators in the co-transfection experiments with the DM2 reporter were significantly different from one another and different activity with Twist or Mad alone (B). (C) Significant activation of the enhancer was observed when Mad and Tkv* or when Twist, Mad, and Tkv* were co-transfected with the DM3 (n = 10) enhancer. (*p<0.05, **p<0.01)

Discussion

Precise regulation of gene activation throughout development is critical for proper formation of many tissues and organs. Since many of the same genes are involved in very different processes, different combinatorial interactions of protein products must be utilized to ensure precision of spatiotemporal expression of any given gene involved in the developmental process (Adryan and Teichmann, 2010). *Mef2* is an example of such a gene that is conserved from invertebrates to vertebrates and varies in spatiotemporal expression regulated by more than a dozen different enhancers throughout development (Black and Olson, 1998). One of the enhancers used in this study is a 1,059 bp enhancer, termed DM1, which controls expression of the *Mef2* gene in mesodermal tissues.

Early mesodermal expression in the developing embryos of DM1 transgenic flies is not as strong as that published by Nguyen and Xu (1998) for a larger 4,285 bp enhancer, suggesting this enhancer is missing some region of the *Mef2* regulatory region necessary for full enhancer expression in the early mesoderm. This region is sufficient to drive expression in the dorsal mesoderm. When dorsoventral patterning occurs in the embryo, *Mef2* expression becomes enriched in the dorsal mesoderm (Nguyen and Xu, 1998), a region that will eventually form the visceral mesoderm, dorsal muscle, and heart (reviewed in Azpiazu *et al*., 1996).

Mef2-lacZ expression was almost entirely abrogated within the mesoderm with an enhancer construct (DM2) that lacks 211 bp of the 3’ end of the DM1 enhancer. This suggests a region between -3,572 and -3,480 is also required for

early mesoderm expression of *Mef2* in addition to the 280 bp region reported by Nguyen and Xu (1998). However, this conclusion is contradicted by the observation that smaller fragments can show mesoderm-specific activity. The DM2 construct may be less active because of a particular combination of binding sites is present that provide a repressor activity; and when larger or small fragments are used that alter this combination of sites the repressor activity is lost. A putative Dorsal binding site is found in the region of the *Mef2* enhancer deleted by DM2, and it is possible that changing from two putative sites to one putative site alters fundamentally the activity of the enhancer. Alternatively, it is possible that the plasmid used for this study was defective in some way. While the enhancer region inserted was sequenced for verification, perhaps a point mutation occurred elsewhere in the plasmid, such as in the *lacZ* gene, which would prevent reporter expression from being observed.

Dorsal is a sequence-specific transcription factor that binds to cis-regulatory elements at the consensus sequence $GGG(T)_{4-5}CC$ (Pan and Courey, 1992). The primary function of Dorsal is activation of genes; however, Dorsal can repress expression of some genes through interactions with co-repressors. The combination of DNA-bound Dorsal and its co-repressors, mostly bHLH proteins, can attract other repressors from the WD40 repeat protein family that do not have DNA binding capabilities but can directly bind Dorsal protein (Dubnicoff *et al.* 1997, Fisher *et al*., 1996, and Neer *et al*., 1994). When an additional 20 bp is deleted from the *Mef2* enhancer (DM3 enhancer), partial *Mef2* expression is restored. Analysis of this region shows the presence of an

additional Dorsal binding site that may be responsible for mediating restriction of *Mef2* from the ventral mesoderm at later stages.

Three E-boxes were found in the enhancer region in this study. Cripps *et al*. (1998) demonstrated the requirement of the E1 site of the enhancer for Twist-mediated expression in the mesoderm and the adult somatic muscle precursors (Cripps *et al*., 1998). In this study, we assessed the importance of the other two E-box sites for their roles in mesodermal *Mef2* expression. Our analysis confirmed that Twist can directly and robustly bind the E1 site and does not bind the E2 site. Both E2 and the E3 binding site were previously untested for direct binding of Twist. Our study shows that Twist can bind the E3 binding site but not as robustly as the E1 site. We mutated the E1 site to test the requirement for this site *in vivo* and also to test whether the E3 binding site can compensate for the loss of the E1 site. Our results show that mutation in the E1 site eliminates *Mef2* expression. This indicates that although Twist is required for *Mef2* expression and can physically bind the E3 site, this site is not necessary for activation of *Mef2* in the developing mesoderm.

The bHLH protein Twist binds to E-box consensus sequences and mediates development of the mesoderm, regulating specification of different cell fates within this lineage. This protein can exist in both homodimer and heterodimer combinations facilitated by the HLH domain and different combinations of homodimer/heterodimer interactions result in differential DNA binding affinity, target preference, and biological activity (reviewed in Castanon *et al*., 2001). The differing abilities of Twist binding to each of the three E-box

binding sites on the *Mef2* enhancer could be indicative of different bHLH factors also being involved in regulating *Mef2*. Perhaps the E2 and E3 sites serve as preferential binding sites for bHLH factors other than Twist to bind *Mef2* and regulate its expression, adding more complexity to the regulation of this enhancer.

The results obtained from the DM1, DM2, DM3, and Twi1 enhancer constructs suggest the Twist and Dorsal (*dl*, FBgn0260632) may work together to activate the *Mef2* enhancer in the mesoderm. Levine and Davidson (2005) have discussed that Dorsal and Twist function in an additive fashion to activate genes in the ventral mesoderm prior to gastrulation. It has also been observed that interactions between Dorsal and bHLH transcription factors, such as Twist, can be either in close proximity or can bind DNA at regions far from one another (Szymanski and Levine, 1995). Twist has also been shown to directly bind the *Drosophila Toll* (*Tl*, FBgn0262473) enhancer, possibly regulating zygotic expression of the Toll receptor (Sandmann *et al*., 2007) which is required for refining Dorsal gradients in other insects, such as *Tribolium castaneum* (Chen *et al*., 2000). It has yet to be shown whether Twist and Dorsal act together to promote *Mef2* expression in the developing mesoderm. If there is an interaction between the two, is the interaction a direct interaction or do the factors bind independently of one another? It is also necessary to determine if Dorsal can bind directly to the *Mef2* enhancer and whether it acts as an activator or repressor of *Mef2*.

Nguyen and Xu (1998) showed the transcription factors Mad and Medea can both physically bind the *Mef2* enhancer at three sites. This study also showed a requirement for Dpp signaling pathway in *Mef2* expression in the mesoderm. What was not determined was whether this dependence on Dpp signaling resulted from the direct binding of Mad/Med to the three binding sites of the enhancer or if Dpp signaling affected the enhancer indirectly. We created a construct with all three Mad/Med binding sites mutated and assessed its expression in the embryo. Our results indicate that this enhancer construct (Mad3) maintained partial expression in the dorsal mesoderm. This could be due to residual expression from earlier stages, as previously suggested by Nguyen and Xu (1998), or may indicate that other transcription factors may bind these Mad binding sites. It has been shown that the Brinker (*brk*, FBgn0024250) protein can compete *in vitro* for binding to Mad sites on the *Ultrabithorax* (*Ubx*, FBgn0003944) enhancer and can prevent Mad from activating Dpp targets *in vivo*. Brinker is also repressed by Dpp signaling (Saller and Bienz (2001). The possibility that this mechanism may be occurring with the *Mef2* enhancer adds complexity to the regulation of the enhancer within mesoderm development.

Due to the requirement for both Twist binding and Mad activity, we sought to determine if these factors interact with one another in cells. Our results showed that the only *Mef2* enhancer activated in the cell culture system was the DM3 enhancer. This enhancer was activated by the presence of Mad with an activated Thickveins receptor and well as by these two proteins in combination with Twist. The results from the cell culture analyses are inconsistent with the

results obtained from our *in vivo* assays. This could be due to the procedure used in our cell culture assays. For example, in these assays, we used a reporter:activator ratio of 9:1. This ratio was the optimized ratio from experiments where the *Actin 57B* (*Act57B*, FBgn0000044) enhancer was activated by MEF2 protein (Kelly Tanaka *et al*., 2008). The mesoderm is specified by morphogen gradients that activate different gene programs in dose dependent manners, leading to variation in the combinations of factors expressed through space and time (Leptin *et al.*, 1991, Xu *et al*., 1998, Sandmann *et al*., 2007, Reeves and Stathopoulos, 2009). It is possible that by using the same 9:1 ratio of reporter:activator, we are not addressing the complexity of the interactions between the various factors involved in *Mef2* regulation. Titrations of the different transcription factors will be necessary to determine if there is a requirement for differential concentrations of transcription factors for activation of the*Mef2* enhancer.

Additionally, as discussed earlier, many other factors could potentially play a role in the expression patterns we observe in embryos by competing for binding sites or by interacting with binding proteins to regulate *Mef2* enhancer expression. These levels of complexity have not been tested in our cell culture system but possibly influence the results of these assays.

Twist activates at least 62 different targets required for mesoderm formation (Sandmann *et al*., 2007). These targets could potentially affect *Mef2* activation through indirect interactions with proteins that can directly bind the enhancer. The necessity for Dpp signaling in regulation of the *Mef2* enhancer

has been demonstrated previously (Nguyen and Xu, 1998) and Mad is capable of activating the enhancer is cell culture. However, mutation of Mad specific binding sites does not abolish expression of *Mef2* in the way *dpp* null mutants do. There is also the possibility that Dorsal protein may be acting to both activate and repress *Mef2* expression. Further optimization of our *Mef2* enhancer for activity in cell culture is necessary before any solid conclusions can be made regarding the interactions of these proteins. It would also be useful to determine if Dorsal binds this enhancer and if any or all of these factors can occupy the enhancer simultaneously.

It is necessary for *Mef2* to be precisely regulated throughout development since it is required for proper mesoderm specification and for differentiation of all lineages of muscle. The full complexity of regulation, while extensively studied, remains poorly understood (reviewed in Black and Olson 1998, reviewed in Ciglar and Furlong, 2009). MEF2 is an evolutionarily conserved protein that affects many cellular and developmental processes from yeast to vertebrates (reviewed in Potthoff and Olson, 2007). Understanding the processes involved in regulating the diverse functions of *Mef2* within *Drosophila* can guide future studies in vertebrate models where redundancy caused by multiple *Mef2* genes can confound analysis.

SUMMARY

Mechanisms of muscle development are conserved in invertebrates and vertebrates. For this reason, *Drosophila melanogaster* is a model organism well suited for the study of such mechanisms. The utility of this model organism also makes it amenable to the types of molecular and genetic analysis that allows researchers to understand the very basal mechanisms involved in these developmental processes from general to cell-specific regulation. The genes that regulate the development of muscle precursors and mature muscle fibers are shown to have functions in other invertebrates and most vertebrate species.

In this dissertation, the gene *CG14614* was identified as a gene required for the formation of the neuromuscular junction between the Tergal depressor of trochanter (TDT) muscle and the Posterior dorsal mesothoracic nerve (PDMN), which innervates this muscle. In the absence of this innervation, as observed in *wings apart* (*wap*) mutants, the TDT muscle degenerates within 24 hours after the onset of metamorphosis.

The protein encoded by *CG14614* exhibits a conserved function in vertebrates. This is demonstrated by the observation that CG14614 protein can functionally rescue a severe craniofacial defect observed in the zebrafish *wdr68* mutant. This is very striking observation since vertebrate craniofacial development occurs in tissues that are absent in *Drosophila*. The protein has also been isolated from rabbit skeletal muscle, complexed with Dyrk proteins that are encoded by genes that also have a *Drosophila* ortholog, *minibrain* (*mbn*). Based upon these observations, it would be interesting to determine if there is a

functional interaction between *CG14614* and *mbn* and if such an interaction is required for proper formation of the neuromuscular junction.

In addition to the identification of *CG14614* as the gene responsible for the *wap* mutation, we were also able to identify the gene *CG14619* as the gene affected by a mutation known as *introverted* (*intro*). This gene is likely an ecdysone response gene and functions in the process of head eversion as well as wing and leg disc extension. This gene may also function in either the development or maintenance of the abdominal muscles, since contractions of the abdominal muscles in response to pulses of ecdysone are required for proper head eversion in the fly.

Regulation of the *Mef2* dorsal mesoderm enhancer was also analyzed for the requirement of interactions of Twist, Mad, and Medea binding. Twist is required for *Mef2* activation. Although a requirement for Dpp signaling has previously been demonstrated for expression of the *Mef2* enhancer, mutation of the binding sites to which Mad and Med bind does not completely abolish expression. The presence of two putative Dorsal binding sites on the enhancer suggest there may be a dual activator-repressor role for Dorsal in the regulation of the mesodermal *Mef2* enhancer. Further investigation is necessary to assess the added complexity of *Mef2* regulation highlighted by this study.

Since the factors regulating specification of the mesoderm and the somatic muscle are conserved across many animal groups, the principles guiding the general developmental process can most likely be extrapolated from simple invertebrate organisms to more complex organisms, such as humans, where

study of these mechanisms is far more challenging and complex. The research presented in this dissertation is intended to shed light on such mechanisms in order to gain a better understanding of both vertebrate muscle formation and the diseases affecting these muscles.

LITERATURE CITED

Adryan, B. and Teichmann, S. A. (2010). The developmental expression dynamics of *Drosophila melanogaster* transcription factors. *Genome Biology*. 11: R40.

Allen, M. J., Shan, X., and Murphey, R. K. (2000). A role for Drosophila Drac1 in neurite outgrowth and synaptogenesis in the giant fiber system. *Molecular and Cellular Neuroscience*. 16: 754-765.

Arbeitman, M. N., Furlong, E. E., Imam, F., Johnson, E., Null, B. H., Baker, B. S., Krasnow, M. A., Scott, M. P., Davis, R. W., and White, K. P. (2002). Gene expression during the life cycle of *Drosophila melanogaster. Science*. 297: 2270-2275.

Artero, R., Furlong, E. E., Beckett, K., Scott, M. P., and Baylies, M. (2004). Notch and Ras signaling pathway effector genes expressed in fusion competent and founder cells during *Drosophila* myogenesis. *Development*. 130: 6257-6272.

Atreya, K. B. and Fernandes, J. J. (2008) Founder cells regulate founder number but not fiber formation during adult myogenesis in *Drosophila*. *Developmental Biology*. 321: 123-140.

Azpiazu, N., Lawrence, P. A., Vincent, J., and Frasch, M. (1996). Segmentation and specification of the *Drosophila* mesoderm. *Genes and Development*. 10: 3183-3194.

Bate, M. (1990). The embryonic development of larval muscles in *Drosophila*. *Development*. 110: 791-804.

Bate, M., Rushton, E. and Currie, D. A. (1991). Cells with persistent *twist* expression are the embryonic precursors of adult muscles in Drosophila. *Development*. 113**:** 79–89.

Baylies, M. K., Martinez-Arias, A., and Bate, M. (1995). *wingless* is required for the formation of a subset of muscle founder cells during *Drosophila* embryogenesis. *Development*. 121: 3829-3837.

Baylies, M. K., and Bate, M. (1996). *twist*: A myogenic switch in *Drosophila*. *Science*. 272: 1481-1484.

Baylies, M. K., Bate, M., and Ruiz-Gomez, M. (1998). Myogenesis: A view from *Drosophila*. *Cell*. 93: 921-927.

Baylies, M. K. and Michelson, A. M. (2001) Invertebrate myogenesis: looking back to the future of muscle development. *Current Opinion in Genetics and Development*. 11: 431-439.

Beltran, S., Blanco, E., Serras, F., Perez-Villamil, B., Guigo, R., Artavanis-Tsakonas, S., and Corominas, M. (2003). Transcriptional network controlled by the trithorax-group gene *ash2* in *Drosophila melanogaster*. *Proceedings of the National Academy of Science*. 100(6): 3293-3298.

Bernstein, S. I., O'Donnell, P. T., and Cripps, R. M. (1993). Molecular genetic analysis of muscle development, structure, and function in Drosophila., pp. 63 - 152 in *International Review of Cytology*. Academic Press, Inc.

Bodmer, R. (1993). The gene *tinman* is required for specification of the heart and visceral muscles in *Drosophila*. *Development*. 118: 719-729.

Black, B. L. and Olson, E. N. (1998). Transcriptional control of muscle development by Myocyte enhancer factor-2 (MEF2) proteins. *Annual Reviews in Cell and Developmental Biology*. 14: 167-196.

Brand, A. H. and Perrimon, N. (1993). Targeted gene expression as a means of altering cell fates and generating dominant phenotypes. *Development*. 118: 401-415.

Buckingham, M. (2006). Myogenic progenitor cells and skeletal myogenesis in vertebrates. *Current Opinion in Genetics and Development*. 16: 525-532.

Campbell, K. P. (1995). Three muscular dystrophies: Loss of cytoskeleton-extracellular matrix linkage. *Cell*. 80: 675-679.

Carpenter, J. M. (1950). A new semisynthetic food medium for *Drosophila*. *Drosophila Information Service*. 24: 96-97.

Castanon, I., Von Stetina, S., Kass, J., and Baylies, M. K. (2001). Dimerization partners determine the activity of the Twist bHLH protein during *Drosophila* mesoderm development. *Development*. 128: 3145-3159.

Chen, E. H. and Olson, E. N. (2004) Towards a molecular pathway for myoblast fusion in Drosophila. *Trends in Cell Biology.* 14: 452-460.

Chen, G., Handel, K., and Roth, S. (2000). The maternal NF-κB/dorsal gradient of *Tribolium castaneum*: dynamics of early dorsoventral patterning in a short-germ beetle. *Development*. 127: 5145-5156.

Ciglar, L. and Furlong, E. E. (2009). Conservation and divergence in developmental networks: a view from *Drosophila* myogenesis. *Current Opinion in Cell Biology*. 21: 754-760.

Cripps, R. M. and Olson, E. N. (1998) Twist is required for muscle template splitting during adult Drosophila myogenesis. *Developmental Biology.* 203: 105-116.

Cripps, R. M., Zhao, B., and Olson, E. N. (1999). Transcription of the myogenic regulatory gene *Mef2* in cardiac, somatic, and visceral muscle cell lineages is regulated by a Tinman-dependent core enhancer. *Developmental Biology*. 215: 420-430.

Cripps, R.M. and Olsen, E.N. (2002). Control of cardiac development by an evolutionarily conserved transcriptional network. *Developmental Biology*. 246: 14-28.

Currie, D.A. and Bate, M. (1991). The development of adult abdominal muscles in *Drosophila*: myoblasts express *twist* and are associated with nerves. *Development*. 113: 91-102.

Demontis, F. and Perrimon, N. (2009) Integration of Insulin receptor/Foxo signaling and dMyc activity during muscle growth regulates body size in *Drosophila*. Development. 136, 983-993.

Deng, X., Ewton, D. Z., Pawlikowski, B., Maimone, M., Friedman, E. (2003). Mirk/dyrk1B is a rho-induced kinase active in skeletal muscle differentiation. *Journal of Biological Chemistry*. 278(42): 41347-41354.

Dubnicoff, T., Valentine, S. A., Chen, G., Shi, T., Lengyel, J. A., Paroush, Z., and Courey, A. J. (1997). Conversion of Dorsal from an activator to a repressor by the global corepressor Groucho. *Genes and Development*. 11: 2952-2957.

Dura, J. M. (2005.12.4). Dura insertions. Personal communication to FlyBase. FBrf0182749.

Dutta, D., Anant, S., Ruiz-Gomez, M., Bate, M., and VijayRaghavan, K. (2004) Founder myoblasts and fibre number during adult myogenesis in *Drosophila*. *Development* 131, 3761-3772.

Eeken, J.C.J., Sobels, F.H., Hyland, V. and Schalet, A.P. (1985). Distribution of MR-induced sex-linked recessive lethal mutations in *Drosophila melanogaster*. *Mutation Research*. 150: 261-275.

Emery, A.E.H. (2002). The muscular dystrophies. *The Lancet*. 359: 687-695.

Fernandes, J., Bate, M., and VijayRaghavan, K. (1991). Development of the indirect flight muscles of *Drosophila*. *Development*. 113: 67-77.

Fernandes, J. J. and VijayRaghavan, K. (1993). Development of indirect flight muscle innervation of *Drosophila melanogaster*. *Development*. 118: 215-227.

Fernandes, J. J., and Keshishian, H. (1998). Nerve-muscle interactions during flight muscle development in *Drosophila. Development*. 125: 1769-1779.

Fernandes, J. J., and Keshishian, H. (2005). Motorneurons regulate myoblast proliferation and patterning in *Drosophila*. *Developmental Biology*. 277: 493-505.

Fernandes, J. J., Atreya, K. B., Desai, K. M., Hall, R. E., Patel, M. D., Desai, A. A., Benham, A. E., Mable, J. L., and Straessle, J. L. (2005). A dominant negative form of Rac1 affects myogenesis of adult thoracic muscles in *Drosophila*. *Developmental Biology*. 285: 11-27.

Fisher, A. L., Ohsako, S., and Caudy, M. (1996). The WRPW motif of the Hairy-related basic helix-loop-helix repressor proteins acts as a 4-amino-acid transcription repression and protein-protein interaction domain. *Molecular and Cellular Biology*. 16(6): 2670-2677.

Fortier, T. M., Vasa, P. P., and Woodard, C. T. (2003). Orphan nuclear receptor βFTZ-F1 is required for muscle-driven morphogenetic events at the prepupal-pupal transition in *Drosophila melanogaster*. *Developmental Biology*. 257: 153-165.

Friedman, A. and Perrimon, N. (2007). Genetic screening for signal transduction in the era of network biology. *Cell*. 128: 225-231.

Furlong, E. M., Andersen, E. C., Null, B., White, K. P., and Scott, M. P. (2001). Patterns of gene expression during *Drosophila* mesoderm development. *Nature*. 293: 1629-1633.

Graveley, B. R., Brooks, A. N., Carlson, J. W., Duff, M. O., Landolin, J. M., Yang, L., Artieri, C. G., van Baren, M. J., Boley, N., Booth, B. W., Brown, J. B., Cherbase, L., Davis, C. A., Dobin, A., Li, R., Lin, W., Malone, J. H., Mattiuzzo, N. R., Miller, D., Sturgill, D., Tuch, B. B., Zaleski, C., Zhang, D., Blanchette, M., Dudoit, S., Eads, B., Green, R. E., Hamonds, A., Jiang, L., Kapranov, P., Langton, L., Perrimon, N., Sandler, J. E., Wan, K. H., Willingham, A., Zhang, Y., Zou, Y., Andrews, J., Bickel, P. J., Brenner, S. E., Brent, M. R., Cherbas, P., Gingeras, T. R., Hoskins, R. A., Kaufman, T. C., Oliver, B., and Celniker, S. E. (2011). The developmental transcriptome of *Drosophila melanogaster*. *Nature*. 471(7339): 473-479.

Guyon, J. R., Steffen, L. S., Howell, M. H., Pusack, T. J., Lawrence, C., and Kunkel, L. M. (2007). Modeling human muscle disease in zebrafish. *Biochimica et Biophysica Acta*. 1772: 205-215.

Haralalka, S. and Abmayr, S. M (2010) Myoblast fusion in Drosophila. *Experimental Cell Research*. 316: 3007-3013.

Hewes, R. S., Schaefer, A. M., and Taghert, P. H. (2000). The *cryptocephal* gene (ATF4) encodes multiple basic-leucine zipper proteins controlling molting and metamorphosis in *Drosophila*. *Genetics*. 155: 1711-1723.

Holm, M., Hardtke, C. S., Gaudet, R., and Deng, X. (2001). Identification of a structural motif that confers specific interaction with the WD40 repeat domain of *Arabidopsis* COP1. *EMBO Journal*. 20(1): 118-127.

Horton, R. M. (1993). *In vitro* recombination and mutagenesis of DNA. *In* "PCR Protocols: Current Methods and Applications" (B. A. White, Ed.). Vol. 15. pp. 251-261. Humana Press, Totawa, NJ.

Jaramillo, M.A.S., Lovato, C.V., Baca, E.M., and Cripps, R.M. (2009). *Crossveinless* and the TGFβ pathway regulate fiber number in the *Drosophila* adult jump muscle. *Development*. 136: 1105-1113.

Kam, Z., Minden, J. S., Agard, D. A., Sedat, J. W., and Leptin, M. (1991). *Drosophila* gastrulation: analysis of cell shape changes in living embryos by three-dimensional fluorescence microscopy. *Development*. 112: 365-370.

Kavlie, R. G., Kernan, M. J., Eberl, D. F. (2010). Hearing in *Drosophila* requires TilB, a conserved protein associated with cilliary motility. *Genetics*. 185(1): 177-188.

Kelly, K. K., Meadows, S. M. and Cripps, R. M. (2002). Drosophila MEF2 is a direct regulator of *Actin57B* transcription in cardiac, skeletal and visceral muscle lineages. *Mechanisms of Development.* 110, 39-50.

Kelly Tanaka, K. K., Bryantsev, A .L. and Cripps, R .M. (2008) Myocyte enhancer factor-2 and Chorion factor-2 collaborate in activation of the myogenic program in Drosophila. *Molecular and Cellular Biology.* 28: 1616-1629.

Keshishian, H., Broadie, K., Chiba, A., and Bate, M. (1996). The *Drosophila* neuromuscular junction: A model system for studying synaptic development and function. *Annual Reviews in Neuroscience*. 19: 545-575.

Khalsa, O., Yoon, J., Torres-Schumann, S., and Wharton, K. A. (1998). TGF-β/BMP superfamily members, Gbb-60A and Dpp, cooperate to provide

pattern information and establish cell identity in the *Drosophila* wing. *Development*. 125: 2723-2734.

Kinstrie, R., Lochhead, P. A., Sibbet, G., Morrice, N., and Cleghon, V. (2006). dDYRK2 and Minibrain interact with the chromatin remodeling factors SNR1 and TRX. *Biochemical Journal*. 398: 45-54.

Kollias, H. D. and McDermott, J. C. (2008). Transforming growth factor-β and myostatin signaling in skeletal muscle. *Journal of Applied Physiology*. 104: 579-587.

Lamminen, A. E. (1990). Magnetic resonance imaging of primary skeletal muscle diseases: patterns of distribution and severity of involvement. *The British Journal of Radiology*. 63: 946-950.

Landgraf, M., Baylies, M., and Bate, M. (1999). Muscle founder cells regulate defasciculation and targeting of motor axons in the *Drosophila* embryo. *Current Biology*. 9: 589-592.

Laurin, M., Fradet, N., Blangy, A., Hall, A., Vuori, K., and Cote, J. (2008). The atypical Rac activator Dock180 (Dock1) regulates myoblast fusion *in vivo*. *Proceedings of the National Academy of Sciences*. 105(40): 15446-15451.

Lee, T. and Luo, L. (1999). Mosaic analysis with a repressible cell marker for studies of gene function in neuronal morphogenesis. *Neuron*. 22: 451-461.

Leptin, M. (1991). *twist and snail* as positive and negative regulators during *Drosophila* mesoderm development. *Genes and Development*. 5:1568-1576.

Leptin, M., Casal, J., Grunewald, B., and Reuter, R. (1992). Mechanisms of early *Drosophila* mesoderm formation. *Development*. 116: 23-31.

Levine, M. and Davidson, E. H. (2005). Gene regulatory networks for development. *Proceedings of the National Academy of Science*. 102(14): 4936-4942.

Lifschytz, E. and Falk, R. (1968). Fine structure analysis of a chromosome segment in *Drosophila melanogaster*. Analysis of X-ray induced lethal. *Mutation Research*. 6: 235-244.

Lifschytz, E. and Falk, R. (1969). Fine structure analysis of a chromosome segment in *Drosophila melanogaster*. Analysis of ethyl methanesulphonate-induced lethals. *Mutation Research*. 8: 147-155.

Lilly, B., Zhao, B., Ranganayakulu, G., Paterson, B. M., Schulz, R. A., and Olson, E. N. (1995). Requirement of MADS domain transcription factor D-Mef2 for muscle formation in *Drosophila*. *Science*. 267: 688-693.

Lin, M-H., Nguyen, H.T., Dybala, D., Stroti, R.V., 1996. Myocyte-specific enhancer factor 2 acts co-operatively with a muscle activator region to regulate Drosophila tropomyosin gene muscle expression. *Proceedings of the National Academy of Sciences*. USA 93, 4623–4628.

Lyons, G. E., Schiaffino, S., Barton, P., Sassoon, D., and Buckingham, M. (1990). Developmental regulation of myosin gene expression in mouse cardiac muscle. *Journal of Cell Biology*. 111: 2427-2436.

Martinez de Lagran, M., Altafaj, X., Gallego, X., Marti, E., Estivill, X., Sahun, I., Fillat, C., and Dierssen, M. (2004). Motor phenotypic alterations in TgDyrk1a transgenic mice implicate DYRK1A in Down syndrome motor dysfunction. *Neurobiology of Disease*. 15: 132-142.

Massague, J., Seoane, J., and Wotton, D. (2005). Smad transcription factors. *Genes and Development*. 19: 2783-2810.

Maqbool, T. and Jagla, K. (2007). Genetic control of muscle development: learning from *Drosophila*. *Journal of Muscle Research and Cell Motility*. 28: 397-407.

McQuilton, P., St. Pierre, S. E., Thurmond, J., and the FlyBase Consortium. (2012). FlyBase 101 – the basics of navigating FlyBase. *Nucleic Acids Research*. 40 (Database issue): D706-714.

Menon, S. D., Osman, Z., Chenchill, K., and Chia, W. (2005). A positive feedback loop between Dumbfounded and Rolling pebbles leads to myotube enlargement in *Drosophila*. *Journal of Cell Biology*. 169(6): 909-920.

Miller, A. (1950). The internal anatomy and histology of the imago of *Drosophila melanogaster*. *In* “Biology of Drosophila” (M. Demerec, Ed.), pp. 420-534. Wiley, New York.

Molina, M. R. and Cripps, R. M. (2001). Ostia, the inflow tracts of the *Drosophila* heart, arise from a genetically distinct subset of cardial cells. *Mechanisms of Development*. 109: 51-59.

Nachtigall, W. and Wilson, D. M., (1967). Neuro-muscular control of Dipteran flight. *Journal of Experimental Biology*. 47: 77-97.

Neer, E. J., Schmidt, C. J., Nambudripad, R., and Smith, T. F. (1994). The ancient regulatory-protein family of WD-repeat proteins. *Nature*. 371: 297-300.

Nguyen, H. T. and Xu, X. (1998). *Drosophila mef2* expression during mesoderm development is controlled by a complex array of cis-acting regulatory modules. *Developmental Biology*. 204: 550-566.

Nissen, R. M., Amsterdam, A., and Hopkins, N. (2006). A zebrafish screen for craniofacial mutants identifies *wdr68* as a highly conserved gene required for endothelin-I expression. *BMC Developmental Biology*. 6: 28-45.

Pan, D. and Courey, A.J. (1992). The same *dorsal* binding site mediates both activation and repression in a context-dependent manner. *The EMBO Journal*. 11(5):1837-1842.

Parks, A. L., Cook, K. R., Belvin, M., Dompe, N. A., Fawcett, R., Huppert, K., Tan, L. R., Winter, C. G., Bogart, K. P., Deal, J. E., Deal-Herr, M. E., Grant, D., Marcinko, M., Miyazaki, W. Y., Robertson, S., Shaw, K. J., Tabios, M., Vysotskaia, V., Zhao, L., Andrade, R. S., Edgar, K. A., Howie, E., Killpack, K., Milash, B., Norton, A., Thao, D., Whittaker, K., Winner, M. A., Friedman, L., Margolis, J., Singer, M. A., Kopczynski, C., Curtis, D., Kaufman, T. C., Plowman, G. D., Duyk, G., and Francis-Lang, H. L. (2004). Systematic generation of high-resolution deletion coverage of the *Drosophila melanogaster* genome. *Nature Genetics*. 36: 288-292.

Patel, N. H. (1994). Imaging neuronal subsets and other cell types in whole-mount *Drosophila* embryos and larvae using antibody probes. *Methods in Cell Biology*. 44: 445-487.

Pinto, B. S., Wilmington, S. R., Hornick, E. E. L., Wallrath, L. L., and Geyer, P. K. (2008). Tissue-specific defects are caused by loss of the *Drosophila* MAN1 LEM domain protein. *Genetics*. 180: 133-145.

Popodi, E., Kaufman, T. C., Holtzman, S. L., Park, S., Carlson, J. W., Hoskins, R. A., Schulze, K. L., Venken, K. J. T., and Bellen, H. J. (2010-). Small X duplications for the stock center collection. Personal communication to FlyBase. FBrf0210621.

Potthoff, M. J. and Olson, E. N. (2007). MEF2: a central regulator of diverse developmental programs. *Development*. 134: 4131-4140.

Prokop, A., Landgraf, M., Rushton, E., Broadie, K., and Bate, M. (1996). Presynaptic development at the *Drosophila* neuromuscular junction: assembly and localization of presynaptic active zones. *Neuron*. 17: 617-626.

Rahman, R., and Lindsley, D. L. (1981). Male-sterilizing interactions between duplications and deficiencies for proximal X-chromosome material in *Drosophila melanogaster*. *Genetics*. 99(1): 49-64.

Ralston, A. and Blair, S. S. (2005). Long-range Dpp signaling is regulated to restrict BMP signaling to a crossvein competent zone. *Developmental Biology*. 280: 187-200.

Rivlin, P.K., Schneiderman, A.M., and Booker, R. (2000). Imaginal pioneers prefigure the formation of the adult thoracic muscles in *Drosophila melanogaster*. *Developmental Biology*. 222: 450-459.

Roy, S., and VijayRaghavan, K. (1999). Muscle pattern diversification in *Drosophila*: the story of imaginal myogenesis. *BioEssays*. 21: 486-498.

Ruiz-Gomez, M., Coutts, N., Price, A., Taylor, M.V., and Bate, M. (2000). *Drosophila* dumbfounded: a myoblast attractant essential for fusion. *Cell*. 102: 189-198.

Rushton, E., Drysdale, R., Abmayr, S.M., Michelson, A.M., and Bate, M. (1995). Mutations in a novel gene, *myoblast city*, provide evidence in support of the founder cell hypothesis for *Drosophila* muscle development. *Development*. 121: 1979-1988.

Saller, E. and Bienz, M. (2001). Direct competition between Brinker and *Drosophila* Mad in Dpp target gene transcription. *EMBO reports*. 21(4): 298-305.

Sambrook, J., Fritsch, E. F., and Maniatis, T. (1989). *Molecular Cloning: A Laboratory Manual*, Ed. 2. Cold Spring Harbor Laboratory Press, Cold Spring Harbor, NY.

Sandmann, T., L. J. Jensen, J. S. Jakobsen, M. M. Karzynski, M. P. Eichenlaub, P. Bork, and E. E. Furlong. 2006. A temporal map of transcription factor activity: mef2 directly regulates target genes at all stages of muscle development. Dev Cell 10:797-807.

Sandmann, T. L., Girardot, C., Brehme, M., Tongprasit, W., Stolc, V., and Furlong, E. E. (2007). A core transcriptional network for early mesoderm development in *Drosophila melanogaster*. *Genes and Development*. 21: 436-449.

Schalet, A. and Finnerty, V. (1968). The arrangement of genes in the proximal region of the X chromosome of *Drosophila melanogaster*. *Drosophila Information Service*. 43: 128-129.

Schalet, A. (1972). New mutants report. *D.I.S.* 49: 36-37.

Schalet, A. and Lefevre, G. (1973). The localization of “ordinary” sex-linked genes in section 20 of the polytene X chromosome of *Drosophila melanogaster*. *Chromosoma*. 44: 183-202.

Schroter, R.H., Lier, S., Holz, A., Bogden, S., Klambt, C., Beck, L., and Renkawitz-Pohl, R. (2004). *kette* and *blown fuse* interact genetically during the second fusion step of myogenesis in *Drosophila*. *Development*. 131: 4501-4509.

Schultz, J.R., Tansey, T., Gremke, L., and Storti, R.V. (1991). A muscle-specific intron enhancer required for rescue of indirect flight muscle and jump muscle function regulates *Drosophila* tropomyosin I gene expression. *Molecular and Cellular Biology*. 11: 1901-1911.

Seoane, J., Le, H.V., Shen, L., Anderson, S.A., and Massague, J. (2004). Integration of Smad and forkhead pathways in the control of neuroepithelial and glioblastoma cell proliferation. *Cell*. 117: 211-223.

Shi, Y., Wang, Y.F., Jayaraman, L., Yang, H., Massague, J., and Pavletich, N.P. (1998). Crystal structure of a Smad MH1 domain bound to DNA: Insights on DNA binding in TGF-β signaling. *Cell*. 94: 585-594.

Shishido, E., Takeichi, M., and Nose, A. (1998). *Drosophila* synapse formation: regulation by transmembrane protein with Leu-rich repeats, *CAPRICIOUS*. *Science*. 280: 2118-2121.

Skurat, A. V. and Dietrich, A. D. (2004). Phosphorylation of Ser^{640} in muscle glycogen synthase by DYRK family protein kinases. *Journal of Biological Chemistry*. 279(4): 2490-2498.

Stapleton, M., Carlson, J., Brokstein, P., Yu, C., Champe, M., George, R. Guarin, H., Kronmiller, B., Pacleb, J., Park, S., Wan, K., Rubin, G. M., Celniker, S. E. (2002). A *Drosophila* full-length cDNA resource. *Genome Biology*. 3(12): R80.

Stute, C., Schimmelpfeng, K., Renkawitz-Pohl, R., Palmer, R.H., and Holz, A. (2004). Myoblast determination in the somatic and visceral mesoderm depends on Notch signaling as well as on *milliways* ($milli^{Alk}$) as receptor for Jeb signaling. *Development*. 131:743-754.

Suganuma, T., Pattenden, S. G., and Workman, J. L. (2008). Diverse functions of WD40 repeat proteins in histone recognition. *Genes and Development*. 22: 1265-1268.

Szymanski, P. and Levine, M. (1995). Multiple modes of dorsal-bHLH transcriptional synergy in the *Drosophila* embryo. *The EMBO Journal*. 14(10): 2229-2238.

Tejedor, F., Zhu, X. R., Kaltenbach, E., Ackermann, A., Baumann, A., Canal, I., Heisenberg, M., Fischbach, K. F., and Pongs, O. (1995). *minibrain*: A new protein kinase family involved in postembryonic neurogenesis in *Drosophila*. *Neuron*. 14: 287-301.

Thummel, C. S. and Pirrotta, V. (1992). New pCaSpeR P element vectors. *Drosophila Information Services*. 71: 150.

Thummel, C. S. (1996). Flies on steroids—*Drosophila* metamorphosis and the mechanisms of steroid hormone action. *Trends in Genetics*. 12(8): 306-310.

Tixier V., Bataillé L. and Jagla, K. (2010) Diversification of muscle types: recent insights from Drosophila. *Experimental Cell Research*. 316: 3019-3027.

Wagner, N., Weyhersmuller, A., Blauth, A., Schuhmann, T., Heckmann, M., Krohne, G., and Samakovlis, C. (2010). The *Drosophila* LEM-domain protein MAN1 antagonizes BMP signaling at the neuromuscular junction and wing crossveins. *Developmental Biology*. 339: 1-13.

Walker, A. R., Davison, P. A., Bolognesi-Winfield, A. C., James, C. M., Srinivasan, N., Blundell, T. L., Esch, J. J., Marks, M. D., and Gray, J. C. (1999). The Transparent Testa Glabra I locus, which regulates trichome differentiation and anthocyanin biosynthesis in *Arabidopsis*, encodes a WD40 repeat protein. *Plant Cell*. 11(7): 1337-1350.

Williams, A. H., Valdez, G., Moresi, V., Qi, X., McAnally, J., Elliott, J. L., Bassel-Duby, R., Sanes, J. R., and Olson, E. N. (2009). MicroRNA-206 delays ALS progression and promotes regeneration of neuromuscular synapses in mice. *Science*. 326: 1549-1554.

Wisotzkey, R.G., Mehra, A., Sutherland, D.J., Dobens, L.L., Liu, X., Dohrmann, C., Attisano, L., and Raftery, L.A. (1998). Medea is a Drosophila Smad4 homolog that is differentially required to potentiate DPP responses. *Development*. 125:1433-1445.

Xu, X., Yin, Z., Hudson, J.B., Ferguson, E.L., and Frasch, M. (1998). Smad proteins act in combination with synergistic and antagonistic regulators to target Dpp responses to the *Drosophila* mesoderm. *Genes and Development*. 12: 2354-2370.